

Prismatic VLMs: Investigating the Design Space of Visually-Conditioned Language Models

Siddharth Karamcheti^{1,2} Suraj Nair² Ashwin Balakrishna² Percy Liang¹ Thomas Kollar^{2,†} Dorsa Sadigh^{1,†}

 github.com/TRI-ML/prismatic-vlms

 github.com/TRI-ML/vlm-evaluation

Abstract

Visually-conditioned language models (VLMs) have seen growing adoption in applications such as visual dialogue, scene understanding, and robotic task planning; adoption that has fueled a wealth of new models such as LLaVa, Instruct-BLIP, and PaLI-3. Despite the volume of new releases, key design decisions around image preprocessing, architecture, and optimization are under-explored, making it challenging to understand what factors account for model performance – a challenge further complicated by the lack of objective, consistent evaluations. To address these gaps, we first compile a suite of standardized evaluations spanning visual question answering, object localization from language, and targeted challenge sets that probe properties such as hallucination; evaluations that provide calibrated, fine-grained insight into a VLM’s capabilities. Second, we rigorously investigate VLMs along key design axes, including pretrained visual representations and quantifying the tradeoffs of using base vs. instruct-tuned language models, amongst others. We couple our analysis with three resource contributions: (1) a unified framework for evaluating VLMs, (2) optimized, flexible code for VLM training, and (3) checkpoints for all models, including a family of VLMs at the 7-13B scale that strictly outperform InstructBLIP and LLaVa v1.5, the state-of-the-art in open-source VLMs.

1. Introduction

If you have built castles in the air, your work need not be lost; that is where they should be. Now put the foundations under them.

— HENRY DAVID THOREAU

[†]Equal Advising ¹Stanford ²Toyota Research Institute
Correspondence to: [<skaramcheti@cs.stanford.edu>](mailto:skaramcheti@cs.stanford.edu)

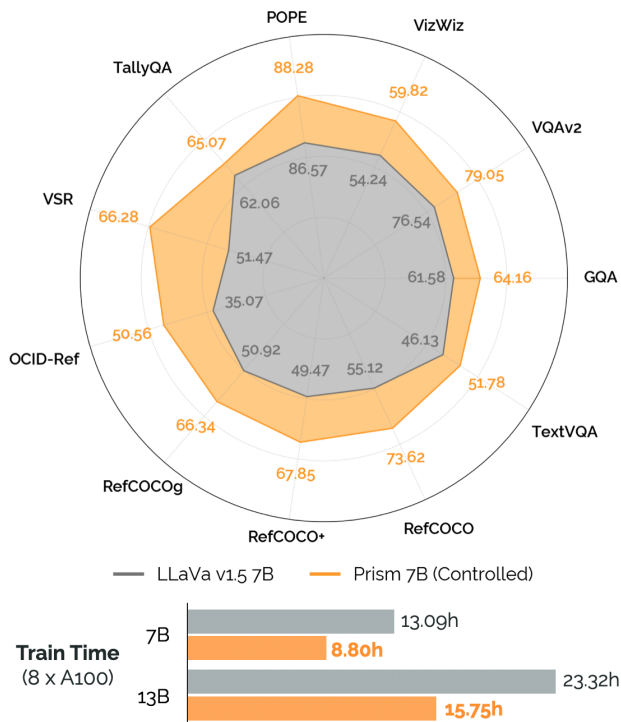


Figure 1. **Prismatic VLMs.*** Through rigorous experiments exploring the design space of visually-conditioned language models (VLMs), we identify insights that improve training. When controlling for data and scale, our models (orange) outperform the state-of-the-art LLaVa v1.5 (gray; Liu et al., 2023b) across 11 diverse tasks, while saving more than 30% the training compute.

Visually-conditioned language models (VLMs) generate natural language responses from image input and text prompts, providing a general, expressive interface for a growing spectrum of applications – grounded chat (Li et al., 2023c; Gong et al., 2023), visual programming (Sur’is et al., 2023; Subramanian et al., 2023), robotic control (Driess et al., 2023; Brohan et al., 2023), etc. This broad adoption is fueled by a recent *paradigm shift* in how we develop VLMs; eschewing the complex architectures and training objectives of prior

***Prismatic** (adj) – relating to or having the form of a prism. Like a geometric prism, our VLMs share a common structure, but are characterized by different “faces” – the individual design axes we explore in this work.

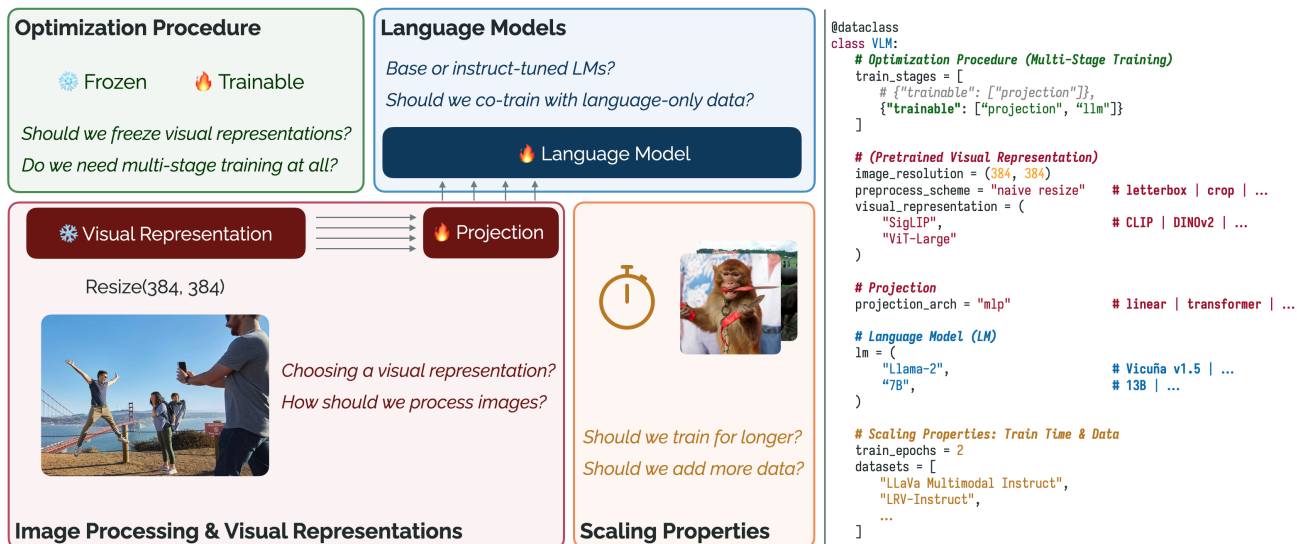


Figure 2. **Exploring VLM Design Axes.** We explore four key design axes for developing VLMs: 1) optimization procedure, 2) image processing and pretrained visual representations, 3) language models, and 4) scaling properties around training time and data (left). To enable this exploration, we make a key resource contribution: an open-source, flexible codebase for efficiently training VLMs (right).

work (Tan & Bansal, 2019; Li et al., 2022; 2023b), new VLMs adopt a simple approach, treat patch features from pretrained visual representations (e.g., CLIP; Radford et al., 2021) as *tokens* that can be projected into the input space of a language model (LM). This “patch-as-token” approach enables training with a simple objective – next-token prediction – and allows us to harness the ecosystem of powerful LMs such as Llama-2 and Mistral (Touvron et al., 2023; Jiang et al., 2023), along with the tools to efficiently train them (e.g., FSDP; Zhao et al., 2023). This combination has fueled the rapid development and release of models such as LLaVa v1.5, and PALI-3 that adopt *the same underlying recipe*, while varying individual ingredients such as the choice of pretrained components, data, or optimization procedure (Liu et al., 2023b; Chen et al., 2023b).

Unfortunately, existing approaches only cover a sliver of the design space around building and training VLMs, without thoroughly evaluating the impact of given choices on downstream capabilities. This motivates the key question of this work: *what are the key design decisions that influence VLM capabilities and downstream use?* To provide answers to this question, we first need a way to **thoroughly evaluate** the strengths and weaknesses of a given model. Doing this effectively requires compiling a standardized evaluation suite comprised of tasks that are diverse and objective; crucially, these tasks should allow for probing specific capabilities such as spatial reasoning, out-of-distribution generalization, and commonsense understanding, amongst others. Second, we need to **rigorously explore** different VLM design axes, not only to build a concrete set of recommendations, but to tie individual choices to downstream performance.

This work addresses these axes through four contributions.

First, to provide fine-grained insight into VLM capabilities, **we compile a standardized evaluation suite** comprised of eleven benchmarks from the vision-and-language literature, including four tasks spanning visual question answering (Bigham et al., 2010; Goyal et al., 2017; Hudson & Manning, 2019; Singh et al., 2019), four tasks spanning object localization (Kazemzadeh et al., 2014; Yu et al., 2016; Wang et al., 2021), and three challenge tasks evaluating fine-grained spatial reasoning, robustness, and hallucination (Acharya et al., 2018; Liu et al., 2022; Li et al., 2023d). Second, **we develop an optimized and modular codebase** for VLM training that emphasizes flexibility, allowing users to easily swap in pretrained components, optimization procedures, data, and more (Fig. 2; right). Third, we use these resource contributions to perform **targeted experiments exploring four key design axes** (Fig. 2; left): 1) optimization procedure, 2) image processing and visual representations, 3) language models, and 4) scaling properties around training time and data. We identify a number of insights; for example, we find that multi-stage training procedures adopted by existing work can be eliminated without impact on performance, reducing compute costs by 20-25%. We also find that *fused* visual backbones that merge features from different backbones such as CLIP (Radford et al., 2021) and DINOv2 (Oquab et al., 2023) lead to more performant VLMs across the board. Finally, we consolidate our findings and efficiently train a family of open-source models – PRISMS – at the 7B/13B scale that **strictly outperform state-of-the-art open VLMs** such as InstructBLIP and LLaVa v1.5.¹

¹We release our optimized training codebase, evaluation suite, and checkpoints for all models trained as part of this work.

github.com/TRI-ML/prismatic-vlms
github.com/TRI-ML/vlm-evaluation

2. Preliminaries

To ground our analysis, we require 1) a VLM model architecture, 2) pretraining data, and 3) a training implementation.

Model Architecture. We adopt the general architecture used by many recent VLMs, such as LLaVa, Qwen-VL, and PaLI-3 (Liu et al., 2023c; Bai et al., 2023; Chen et al., 2023b). These architectures use a (pretrained) visual backbone to map an input image to a sequence of patch features that are then projected individually into the embedding space of an LM. Formally, a VLM takes as input an image $x_{\text{img}} \in \mathbb{R}^{H \times W}$ and text prompt tokens u_{prompt} with arbitrary sequence length K . These inputs are then fed to the following components: 1) a visual representation backbone, 2) a vision-language projector, and 3) a language model.

Visual Representation. We first process x_{img} subject to a visual representation backbone V_{ω} that outputs a sequence of features $p_{\text{img}} \in \mathbb{R}^{L \times h_{\text{vision}}}$ where $p_{\text{img}} = V_{\omega}(x_{\text{img}})$. As an example, p_{img} might be the patch features output by a Vision Transformer (ViT; Dosovitskiy et al., 2021).

Vision-Language Projector. Next, we map p_{img} to a sequence of embeddings $e_{\text{img}} \in \mathbb{R}^{L \times h_{\text{text}}}$ via a learned projector F_{ψ} , where $e_{\text{img}} = F_{\psi}(p_{\text{img}})$.

Language Model. Finally, we concatenate the sequence e_{img} with the text prompt embeddings $e_{\text{prompt}} = \text{embed}(u_{\text{prompt}})$, passing the result to the language model. The language model generates output text $u_{\text{gen}} = \text{LM}_{\theta}([e_{\text{img}}; e_{\text{prompt}}])$.

The composition $\text{LM}_{\theta}([F_{\psi}(V_{\omega}(o_{\text{rgb}})); \text{embed}(u_{\text{prompt}})])$ then defines a VLM. Given a triple $(x_{\text{img}}, u_{\text{prompt}}, \hat{u}_{\text{gen}})$ during training, we minimize the loss $\mathcal{L}(\omega, \psi, \theta) = -\log p(\hat{u}_{\text{gen}} | x_{\text{img}}, u_{\text{prompt}})$ via gradient descent.

Pretraining Dataset. We limit our selection of pretraining data to datasets that are fully open-source (e.g., under permissive research licenses), and that have been used in prior work. Specifically, we use the LLaVa v1.5 data mixture, which consists of two subsets used for a multi-stage training pipeline. The first subset consists of a 558K sample mixture of examples sourced from various captioning datasets (e.g., Conceptual Captions, LAION Sharma et al., 2018; Schuhmann et al., 2021), while the second consists of 665K *multimodal instruct tuning examples* comprised of synthetic data generated in Liu et al. (2023c), as well as examples from existing vision-language training sets (e.g., GQA, TextCaps; Hudson & Manning, 2019; Sidorov et al., 2020), and notably, a sample of language-only data from ShareGPT (ShareGPT, 2023). We provide a comprehensive breakdown of the pretraining data mixture in §A.1.

Training Implementation & Verification. To investigate the design axes enumerated in §1, we require code for VLM training that is *efficient* and *flexible*; critically, we need the ability to easily swap out vision and LM backbones and

handle arbitrary optimization procedures (e.g., freezing the vision backbone during training). With these requirements, we implement our training codebase in PyTorch, using Fully Sharded Data Parallel (FSDP; Zhao et al., 2023) and BF16 mixed precision. FSDP lets us specify precision for individual model components (e.g., FP16 for vision backbones, BF16 for LMs), enables portability to different hardware, and provides minimal implementation overhead. Following reproducibility practices from prior work (Karamcheti et al., 2021; Biderman et al., 2023), we fix initialization randomness and fix batch order during training. We leverage TIMM (Wightman, 2019) and Hugging Face Transformers (Wolf et al., 2019) to provide pretrained models.

To validate our code, we run an apples-to-apples reproduction of LLaVa v1.5 (Liu et al., 2023b) at both the 7B and 13B parameter scale. Successful reproduction results are in Fig. 4 (left). We find our implementation is considerably more efficient than the reference LLaVa v1.5 training implementation: when benchmarked on the same hardware (an AWS p4de.24xlarge node with 8 A100 GPUs), we observe 20% faster step times with our FSDP-backed implementation, a notable gain given LLaVa leverages the well-optimized DeepSpeed ZeRO library (Rasley et al., 2020).

We highlight this open-source training codebase as one of the key contributions of this work. Unlike other open codebases, we provide a modular and expressive interface for easily specifying or adding model components, optimization procedures, and data with minimal code changes (Fig. 2; right). In providing an *efficient* and *easily extensible* framework, we enable future research around designing new evaluations, developing and training new VLMs, and finetuning or otherwise adapting existing models for diverse downstream applications – all while maintaining a high standard of reproducibility and controlled experimentation.

3. Evaluation Suite

The first contribution of this work is a unified evaluation suite that offers *fine-grained insight* into the capabilities of a given VLM. Recent work in evaluating VLMs tends to rely on automated evaluations that use powerful LMs such as GPT-4 (OpenAI et al., 2023) to judge *relative and subjective performance* (Liu et al., 2023e; Yu et al., 2023), making it hard to measure the absolute impact of a given design change. Instead, we focus on evaluations with well-defined metrics, spanning the following three areas:

Open-Ended Visual Question Answering. We evaluate on VizWiz (Bigham et al., 2010), VQAv2 (Goyal et al., 2017), GQA (Hudson & Manning, 2019), and TextVQA (Singh et al., 2019). Both VizWiz and VQAv2 assess general visual reasoning; VizWiz also contains a series of *unanswerable* questions. GQA evaluates spatial reasoning, while

Open-Ended Visual Question Answering

VQA_{v2}:
General Visual Reasoning



Q: What brand name is on cooler to the left? A: Coca-Cola

GQA:

Spatial Reasoning



Q: What animal is sitting on the sidewalk? A: Bear

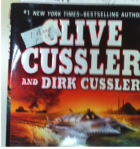
TextVQA:
Text Reasoning



Q: What is the price of the bananas per kg? A: \$11.98

VizWiz:

Unanswerable Questions



Q: What is the name of this book? A: Unanswerable

Localization

RefCOCO+/_g:

Grounding Common Objects/Attributes



Guy in white shirt. [0.39, 0.15, 0.7, 0.79]

OCID-Ref:

Complex Grounding in Clutter



The mint toothpaste on the rear right [0.6, 0.37, 0.66, 0.52]

Challenge Sets

VSR:

Spatial True/False



The cow is ahead of the person. False

TallyQA:

Counting



Q: How many dogs are to the left of the person? One

POPE:

Probing Hallucination



Q: Is there a person in the image? No

Figure 3. Evaluation Suite Overview. We compile multiple established benchmarks spanning visual question answering, localization, and challenge tasks (e.g., evaluating counting, spatial relationships, propensity to hallucinate). This evaluation suite forms the backbone for all of our analysis, giving us fine-grained insight into the impact of individual VLM design choices.

TextVQA assesses reasoning around text (e.g., labels, signage) present in an image.

Localization. Part of the pretraining data mixture (from §2) contains examples of predicting normalized bounding box coordinates given referring expressions in language. As such, we evaluate bounding box prediction accuracy on RefCOCO, RefCOCO+, and RefCOCOg (Kazemzadeh et al., 2014; Yu et al., 2016), and on OCID-Ref (Wang et al., 2021). RefCOCO focuses on short descriptions with spatial anchors, RefCOCO+ on strictly appearance based descriptions, and RefCOCOg on long, rich descriptions; OCID-Ref is a robotics dataset probing out-of-distribution generalization, with a focus on localizing objects in clutter.

Challenge Sets (Closed-Set Prediction). We evaluate on Visual Spatial Reasoning (VSR; Liu et al., 2022), TallyQA (Acharya et al., 2018), and POPE (Li et al., 2023d). VSR consists of challenging True/False questions about individual spatial relationships in diverse scenes (e.g., “the cake is at the edge of the dining table”); this is an especially challenging task, with most existing models failing to outperform the majority class baseline (51%). TallyQA consists of questions that assess a VLM’s ability to count objects described in language, with expressions that range in complexity. Finally, POPE consists of targeted Yes/No questions that assess a VLM’s propensity to hallucinate.

We use the *validation* sets for all benchmarks except GQA (where we use the recommended test-dev split), VSR (where we use the zero-shot test split), and POPE (where there is only a single evaluation split). We provide further detail around evaluation protocols in Appx. B.

4. Experiments – Investigating Design Axes

Our second contribution is a series of targeted experiments exploring the VLM design space along *four key axes*: (§4.1) optimization procedure, (§4.2) image processing and visual representations, (§4.3) language models, and (§4.4) scaling properties such as training time and data diversity.

Experiment Design: Protocols & Drawing Conclusions.

We first validate our VLM training implementation by reproducing LLaVa v1.5 (see §2), adopting the design choices of the original work – the same choices used by many other recent VLMs: “letterbox padding” to process images, CLIP ViT-Large with a patch size of 14 and input resolution of 336px (CLIP ViT-L/14 @ 336px; Radford et al., 2021) as the visual representation, Vicuña v1.5 as the LM backbone, and the two-stage training pipeline using both data subsets described in §2. Successful reproduction results at both the 7B and 13B scale are in Fig. 4 (left). Given both the fidelity of our reproduction and the prevalence of these design choices, we anchor our analyses around this parameterization. Critically, each of the experiments in §4.2, §4.3, and §4.4 are formulated as *single-step changes of this base architecture, with all other choices held constant*.

As each evaluation in §3 uses different metrics with different scales, direct comparison is challenging. We address this by computing normalized Z-scores for each model and evaluation (using the mean and standard deviation across all models). These scores are used to compute statistical significance (further details in §B.2), and to set the relative scales of each radar plot (for completeness, we also provide the absolute metrics as colored and bolded labels).

Investigating the Design Space of Visually-Conditioned Language Models

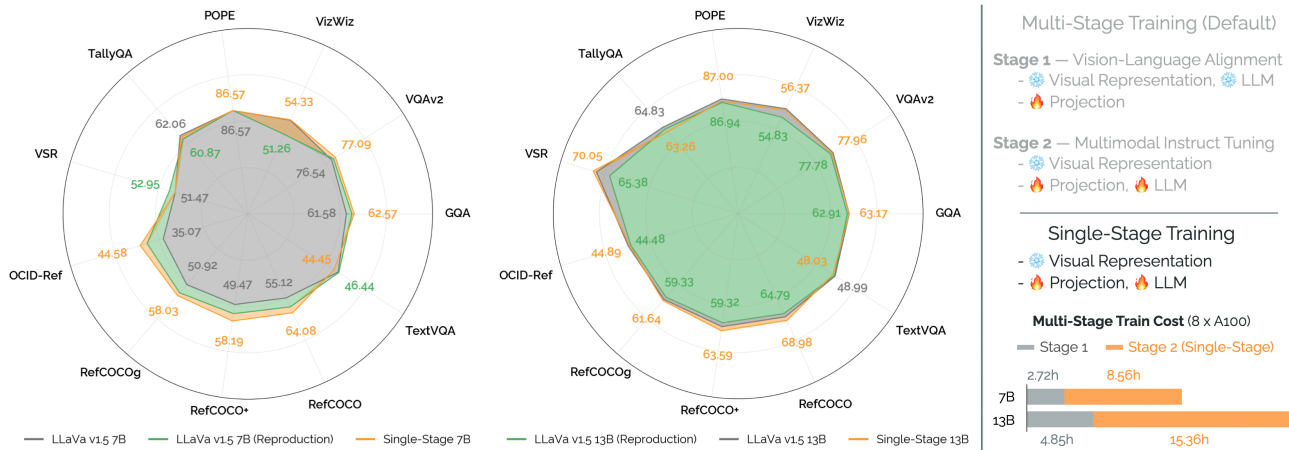


Figure 4. Reproducing LLaVa v1.5 & Exploring Optimization Procedures. To validate our training codebase (§2), we reproduce LLaVa v1.5 (green), with our models reproducing the performance reported in Liu et al. (2023b) (gray). We then run our first experiment (§4.1) investigating the need for expensive multi-stage training (right). We find that single-stage training produces VLMs that maintain or outperform multi-stage models (orange), saving considerable compute; as a result, we carry this change forward to all future experiments.

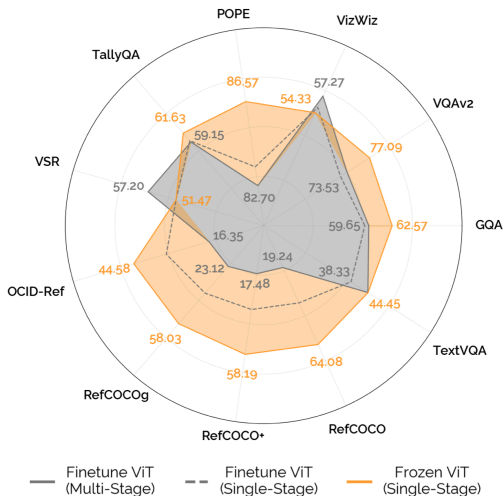


Figure 5. Full Finetuning through Visual Backbones. We explore the impact of finetuning the (conventionally frozen) visual backbone in addition to the projector and language model during training. We see that in both the single and multi-stage paradigms, finetuning the vision backbone dramatically degrades performance across almost all benchmarks – especially on localization tasks.

4.1. Optimization Procedure

In this section we focus on design choices around the optimization procedure used to initialize and train each of the three components described in §2. Specifically, we examine the effects of multi-stage training where different VLM components are frozen at different points in training.

Multi-Stage Training. One of the prevalent design choices adopted by many VLMs (Chen et al., 2023a; Ye et al., 2023) is the inclusion of a two-stage training pipeline: (1) an *alignment* stage to align vision and language features by training the randomly initialized projector F_ψ in isolation, freezing all other components (Fig. 4, right) and (2) a *finetuning*

stage, where only the visual representation is frozen while both the projector and LM are trained.

Adopting multi-stage training complicates implementation and adds to training cost; therefore, as an initial experiment, we evaluate the need for this first stage through a targeted ablation. We compare the default two-stage training procedure with a *single-stage* approach that skips directly to finetuning F_ψ and the LM. We find (Fig. 4; left) that including the explicit projector pretraining stage is *unnecessary*, with single-stage training improving aggregate performance ($p = 0.007$). Eliminating this first stage saves 20-25% of training cost, and removes the need for additional, stage-specific data (e.g., the captioning subset from §2). *As this change strictly improves performance and efficiency, we adopt single-stage training for all following experiments.*

Full Finetuning through Visual Backbones. Another popular design choice in existing VLMs that leverage pretrained visual representations is to leave the visual backbone *frozen* during the entirety of training (Liu et al., 2023b; Driess et al., 2023; Li et al., 2023b). Such a choice limits the potential to learn improved visual representations conducive to language generation during the course of training. Thus, we ask – *is there potential to improve VLM performance by finetuning the full model, including the visual backbone?* We find (Fig. 5) that this is not the case, and that finetuning the visual backbone *significantly degrades performance* ($p = 0.00407$), especially on tasks requiring fine-grained spatial reasoning such as RefCOCO and OCID-Ref.

Remark. The degraded performance from full finetuning could be for a number of reasons ranging from the scale and diversity of the vision-language data we train on to language generation as a learning objective (vs. objectives that encourage learning fine-grained perceptual features). Especially given the existence of closed-source models such

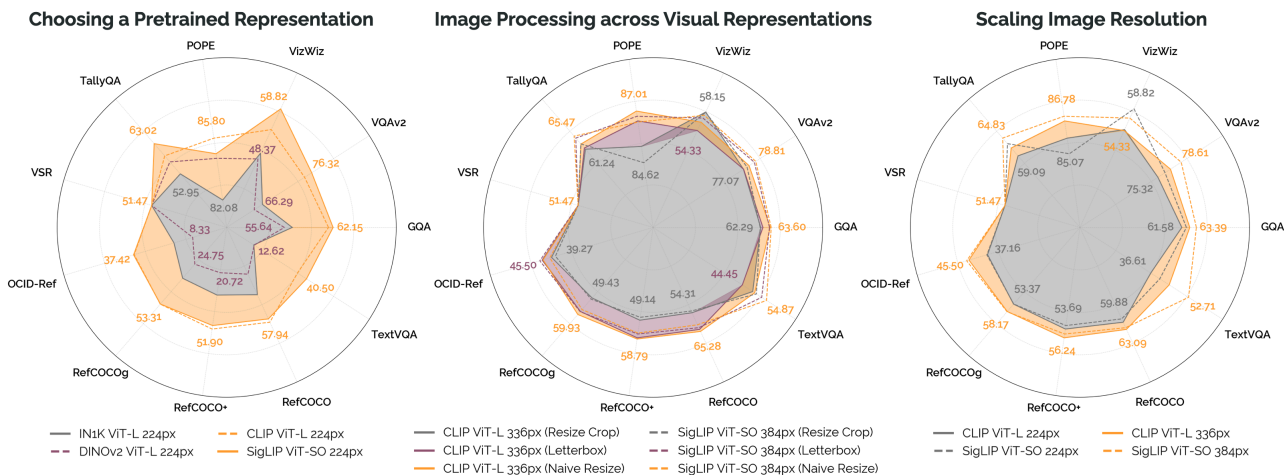


Figure 6. **Image Processing & Visual Representations.** We explore choices around image processing and visual representations in §4.2. Specifically, we investigate the impact of different visual representations (**left**), how performance varies as function of image processing strategies (**middle**), and the impact of increasing input image resolution (**right**).

as Fuyu-8B (AI, 2023) that adopt this paradigm to great success, we believe that identifying ways to prevent such feature collapse during VLM training (e.g., via auxiliary objectives) to be a rich direction for future work.

4.2. Image Processing & Visual Representations

Choosing a Pretrained Vision Representation. CLIP (Radford et al., 2021) has become the default choice for visual representation for almost all VLMs, despite a wealth of visual representations trained on diverse data sources. In this experiment, we perform a head-to-head comparison between CLIP, SigLIP (Zhai et al., 2023), DINOv2 (Oquab et al., 2023), and a standard Vision Transformer pretrained for classification (on ImageNet-21K, finetuned on ImageNet-1K; Dosovitskiy et al., 2021; Steiner et al., 2021); for fair comparison, we use the ViT-Large². We find (Fig. 6; left) that the backbones trained with vision-language contrastive objectives (i.e., CLIP and SigLIP) are significantly more performant than alternatives ($p = 8.88e-8$).

Remark. While the vision-language contrastive objective is one explanation for the strengths of CLIP and SigLIP, another possible explanation is one of training image distribution. Both CLIP and SigLIP contain internet-sourced images (e.g., sketches, diagrams, animated graphics, etc.) not in ImageNet or in the DINOv2 pretraining data.

Image Processing across Visual Backbones. Most images have resolutions and aspect ratios that widely vary, yet most visual backbones expect square images at a fixed size; to reconcile this, the overwhelming default is to “resize & crop” an image to size. While this tends to work well for applica-

tions such as classification, cropping out parts of an image is especially harmful for tasks requiring full-scene reasoning. In this experiment, we evaluate three different image processing schemes – the default “resize & crop” scheme, the “letterbox padding” scheme used by LLaVa v1.5 that pads non-square images to square, and a “naive resize” scheme that warps the original image aspect ratio, squeezing or stretching an image to square. Our findings (Fig. 6; middle) are surprising: while cropping is clearly suboptimal, the “naive resize” scheme is the most performant for CLIP. For SigLIP, both “naive resize” and “letterbox padding” perform similarly. In general, our results favor “naive resizing” over “letterbox padding” but we cannot rule the improvement statistically significant ($p = 0.0148$).

Remark. Two speculative arguments for naively resizing an image over padding are those of minimizing “dead pixels” and distribution shift. An image with a 16:9 aspect ratio that is padded to square introduces a large amount of uninformative pixels (exceeding 40%); warping the aspect ratio is possibly less of a shift. Coupled with the innate patch dimensionality of a Vision Transformer ($d = 1024$ for a 16×16 pixel patch), naively resizing an image may preserve enough information for the downstream LM (with 7B+ parameters) to extract the properties necessary for downstream tasks.

Scaling Image Resolution. Another trend in recent VLMs is increasing input image resolution with the hope of capturing fine-grained details that improve downstream performance (Liu et al., 2023b; Li et al., 2023a). Our findings (Fig. 6; right) confirm this hypothesis, with scaling to 336px or 384px offering significant improvements ($p = 5.66e-4$).

Remark. While scaling up image resolution seems like a clear win, we caution that it comes with a significant increase in compute complexity for VLMs that project individual ViT patches into the embedding space of an LM.

²To evaluate on an image resolution common to all representations (224px), we use the *shape-optimized* SigLIP model (ViT-SO Alabdulmohsin et al., 2023) that is slightly larger than a ViT-Large at 400M parameters (vs 307M).

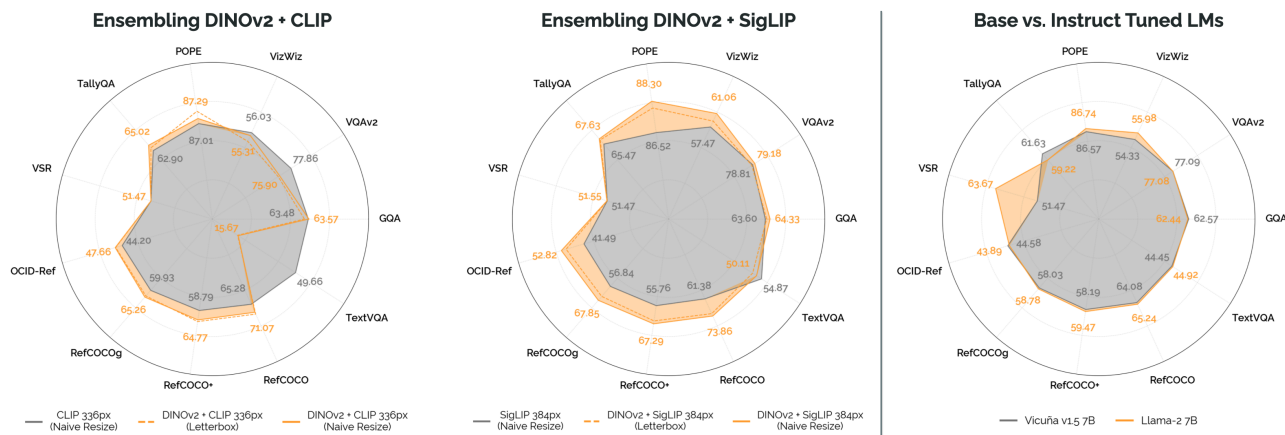


Figure 7. Ensembling Different Visual Representations & Base vs. Instruct-Tuned LMs. We explore fusing visual features from DINOv2 and CLIP/SigLIP models, and find that doing so significantly boosts performance on localization and challenge evaluations (left). We additionally evaluate the differences between base (Llama-2; orange) and instruct-tuned (Vicuña v1.5; gray) language models (right); we find that Llama-2 offers similar quantitative performance, while being less prone to hallucination (Fig. 11).

Assuming a fixed patch granularity, doubling the input resolution results in *four times the number of input patches* fed to the LM. Coupled with the quadratic cost of traditional Transformer attention as a function of sequence length, this is a sixteen-fold increase in time complexity (with a comparable explosion in memory requirements).

Ensembling Different Visual Representations. A rich body of prior work in vision identifies that different types of visual representations trained with different inductive biases can lead to improved performance for a broad spectrum of applications (Kobayashi et al., 2022; Karamcheti et al., 2023). Motivated by this, we ask if this same trend holds true for VLM training – specifically whether ensembling DINOv2 features with vision-language contrastive features from CLIP and SigLIP can lead to improved performance, following the approach taken in Kerr et al. (2023). To implement this efficiently, we simply concatenate patch features from different backbones along the channel dimension for each patch, resulting in the *same number of input patch embeddings*, just with double the feature dimension. To adjust for this, we just increase the input dimension to our projector F_ψ (a 2-layer MLP) at negligible cost. We find (Fig. 7 - left) that fusing DINOv2 and SigLIP features provides significant gains across the board ($p = 0.00162$), with a notable exception for the DINOv2 + CLIP models ($p = 0.4066$), where combining DINOv2 features seem to be particularly harmful on TextVQA. Looking at the remaining results, we see especially impressive gains of 5-10% on localization and challenge tasks; in general, the DINOv2 + SigLIP fused representations are the most performant visual representations we try, with virtually no added parameters.

Remark. Following the hypotheses in Kerr et al. (2023) and similar work, we believe that DINOv2 features provide features that capture low-level spatial properties of an image, augmenting the higher-level “semantic” properties captured

by vision-language contrastive models. We note that this conclusion may generalize beyond DINO-style backbones; the only reason we do not evaluate the fusion of ImageNet and CLIP/SigLIP backbones as well is due to a mismatch in patch granularity (the ImageNet backbone uses a patch granularity of 16×16 vs. the 14×14 granularity used by all other backbones). We believe that further exploring the impact on these type of fused, multi-resolution features for VLMs is a compelling avenue for future work.

4.3. Integrating Language Models

Base vs. Instruct-Tuned LMs. Instruct tuning (or chat tuning; Ouyang et al., 2022; Chung et al., 2022) is a way to finetune base LMs (trained for next-token prediction) to behave as dialogue agents, offering a natural input/output interface for a wide spectrum of applications. As a result, instruct tuned models like Vicuña (Zheng et al., 2023) have become the default backbone for VLMs. Unfortunately, instruct tuning has drawbacks, introducing bias and regressions in performance (Ouyang et al., 2022). Thus, in this experiment we evaluate the impact of instruct-tuned LM backbones on downstream VLM performance via a head-to-head comparison between a base LM (Llama-2; Touvron et al., 2023), and an instruct-tuned variant (Vicuña v1.5). We find (Fig. 7 - right) that instruction-tuned LMs *yield no statistically significant improvement in performance over base LMs* ($p = 0.373$), but *differ in qualitative performance*. Specifically, we observe that instruct-tuned LMs lead to VLMs that are more verbose, prone to hallucination, and generally less specific in their responses (Fig. 11).

Co-training on Language-only Safety Data. The LLaVa v1.5 pretraining dataset we use for training consists of 40K examples of language-only data sourced from ShareGPT (ShareGPT, 2023); this data consists of a diverse set of user-uploaded conversations with OpenAI’s ChatGPT; cru-

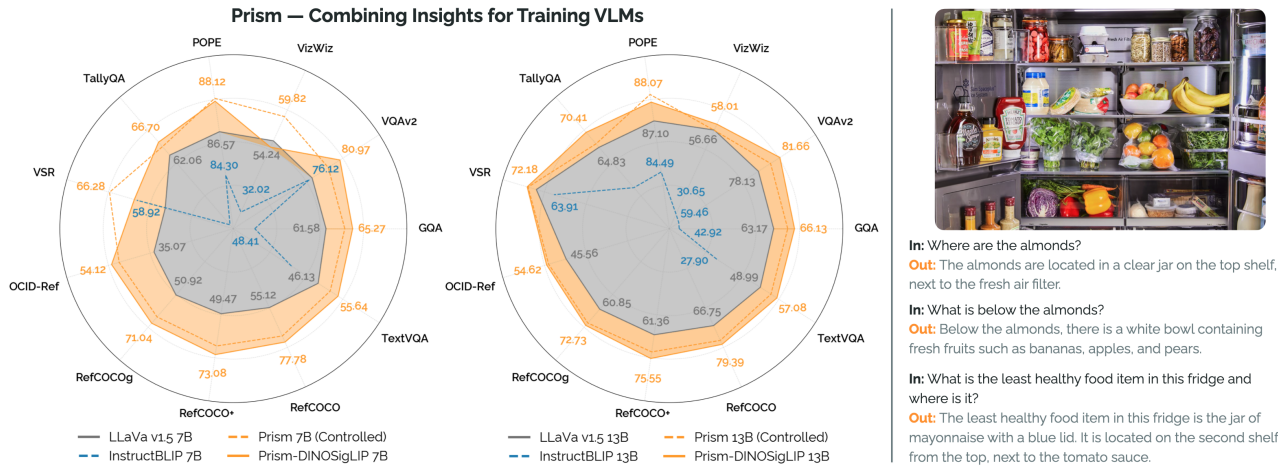


Figure 9. **PRISM: Combining Insights for Training VLMs.** We distill our experimental results from §4 into a series of key insights for training VLMs. Our resulting family of VLMs – PRISMs – adopt 1) single-stage training pipelines, 2) fused DINOv2 and SigLIP representations with naive image resizing, 3) base LMs, and 4) train on multiple data sources, for two epochs.

4) *Scaling Properties:* Adding diverse data and extending training time significantly boost performance.

As a final step, we combine these insights to inform a new family of VLMs – PRISMs – at the 7B and 13B parameter scale. We present results comparing our DINOv2 + SigLIP PRISM models to InstructBLIP and LLaVa v1.5 in Fig. 9. We additionally run a head-to-head comparison against LLaVa v1.5, training a model – PRISM (Controlled) – given the exact same data and training budget. Both sets of PRISM models uniformly outperform both baselines by large margins across our evaluation suite, with strong qualitative performance (Fig. 9; right).

6. Limitations & Future Work

While this work focuses on rigorously studying VLM design choices, there are two key limitations in our approach. Of primary concern is the generality of our model architecture; while the three component architecture we define in §2 is reflective of the majority of existing VLMs, there are other architecture innovations and optimization procedures that our study does not currently capture; as a notable example, we do not study the Perceiver-based architectures used by models such as Flamingo or IDEFICS (Alayrac et al., 2022; Laurençon et al., 2023) for interleaved image-text training. Though many of our takeaways are general (e.g., these models also use contrastive backbones such as CLIP, and autoregressive LMs), there remain open questions as to the extent our findings transfer to different architectures or at larger scale (e.g., 70B LMs).

A separate limitation is that of evaluation; we make the intentional choice in this work to focus on standardized evaluations, with objective metrics. While this lets us probe fine-grained capabilities, we do not capture the scope of the dyadic interactions afforded by existing VLMs – the

ability to carry on extending dialogues that flit across topics grounded in a visual context. While some of the automated evaluations discussed in §3 provide initial steps for evaluating these open-ended behaviors, future work will investigate how to extend such evaluations to longer, richer contexts. Related to this are the downstream applications built on top of broadly capable VLMs – applications such as using VLMs to learn robotic control policies or for visual programming (Brohan et al., 2023; Sur’is et al., 2023); a compelling avenue for future work is understanding how to co-design VLMs with the downstream applications to boost the performance of both the upstream VLM, and downstream system.

7. Conclusion

We present a rigorous investigation of the design space of visually-conditioned language models, distilling key insights for training future models. This investigation is enabled by two key resource contributions: 1) an evaluation suite that enables *fine-grained insight* into a VLM’s capabilities, and 2) an optimized, extensible codebase for training VLMs with an emphasis on *flexibility* – flexibility over optimization procedures, image processing and visual representations, language models, and scaling. Our insights allow us to train a family of VLMs – PRISMs – that outperform state-of-the-art open VLMs such as InstructBLIP and LLaVa-v1.5. However, these models are secondary to the central goal of this work – *establishing a foundation for future work in training and evaluating VLMs*. We hope that our investigation and resources serve as a starting point; a template for reasoning about what matters in developing the next generation of broadly capable VLMs.

Broader Impacts

We take the established position that building visually-conditioned language models in the open – with open data, open (and efficient) training code, and open evaluation code – is strictly beneficial for the broader machine learning community and the public (Zellers et al., 2019; Touvron et al., 2023). Being transparent and ensuring that our work is accessible to all stakeholders is key to mitigating risks and empowering the positive use of VLMs. To this end we discuss the harms of our work, and VLMs more broadly over the following paragraphs, in addition to making several open source resource contributions: (1) A codebase for efficient, optimized VLM training. (2) An evaluation suite for evaluating fine-grained VLM capabilities. (3) The complete set of pretrained model checkpoints for *all* VLMs trained in this work – including those with *known racist and toxic behavior* from Fig. 8.

7.1. Risks and Known Biases

Visually-conditioned language models inherit all of the risks and biases associated with language models (Touvron et al., 2023; Brown et al., 2020), *as well as* with underlying vision models and corresponding pretraining datasets (Schuhmann et al., 2021; Lin et al., 2014).

Toxic and Unsafe Outputs. As shown in Fig. 8, VLMs are capable of generating toxic and unsafe content. This is true with and without “safeguards” in place (e.g., safety tuning data). As we mention in §4.3, our exploration in this work is cursory, but reveals the potential for generating racist, sexist, abusive, and otherwise unsafe language. While including safety-tuning data in the training mix is one low-effort way to prevent the ease of generating toxic content (at minimal cost to performance as we show in our work), it is not enough. VLMs are especially vulnerable to adversarial or even out-of-distribution *image inputs* that may inadvertently trigger unsafe output (Qi et al., 2023; Liu et al., 2023d). We hope that the accessibility of our training code and models enables future research in mitigating such problems.

Western Bias & (American) English Bias. The data and pretrained language models used in this work reflect a heavy bias towards American English and corresponding cultural norms. While the LMs we use in this work are exposed to some multilingual data (with our VLMs showing some ability to handle simple phrases in languages such as Spanish, French, and Chinese), a key limitation is in our *visual* data diversity. Our pretraining images are sourced from datasets such as COCO (Lin et al., 2014), sourced primarily from (English) subsets of Flickr.

Factuality, Hallucination, & Reliability. A known limitation of both LMs and VLMs is that of factuality and hallucination; for VLMs this is especially problematic, as

models tend to “imagine” objects or properties of a scene that are then reinforced over subsequent interactions. For this reason, we include both VizWiz (Bigham et al., 2010) and POPE (Li et al., 2023d) in our evaluation suite; VizWiz has a series of commonsense questions and *unanswerable questions* that are explicitly used to probe model reliability. POPE is a benchmark specifically created to evaluate hallucination at different difficulties (e.g., when asked about adversarial objects that have strong co-occurrence with the type of scene depicted in an image, generally popular objects, etc.). We hope that by including these tasks as part of our evaluation suite, future VLMs move towards making design choices that lead to reduced hallucination and improved reliability (and vice-versa).

7.2. Benefits and Potential Opportunities

In §1 and §6, we discuss applications where VLMs are already making a positive impact, accelerating research in areas such as robotics, visual programming and more. Here, we speak specifically as to the benefits and opportunities that our work – specifically our resource contributions – provide for the broader research community.

Training and Finetuning Accessibility. One of the key benefits of our VLM training codebase is its efficiency; to fully train a 7B parameter VLM (e.g., PRISM 7B (Controlled); Fig. 9), takes less than 9 hours on 8 A100 GPUs, with finetuning and evaluation possible on individual GPUs (or even CPU); this is in sharp contrast to existing codebases for VLM training that are far less efficient. Reducing the barrier to entry for trying new ideas around VLM development is key to enabling progress in risk mitigation, robust evaluation, and integration for downstream applications. Furthermore, the *flexibility* of our training codebase enables swapping in smaller, more compute-efficient components (e.g., new LMs at the 1B scale).

Extending our Evaluation Suite. Our evaluation suite is written in a way that makes it easy to add and evaluate new VLMs, *as well as* add new tasks. It is our plan to continually extend our suite with new evaluations (especially those probing for bias, toxicity, hallucination, and other unsafe or undesirable behaviors), as they are released.

Acknowledgements

Toyota Research Institute (“TRI”) provided funds to support this work. Siddharth Karamcheti is grateful to be supported by the Open Philanthropy Project AI Fellowship. Finally, we would like to thank Adrien Gaidon, Rares Ambrus, Achal Dave, Blake Wulfe, Masha Itkina, Jean Mercat, Igor Vasiljevic, Sedrick Keh, Kushal Arora, John Thickstun, and David Hall for their insight and advice during the early development of this work.

References

- Acharya, M., Kafle, K., and Kanan, C. TallyQA: Answering complex counting questions. In *Association for the Advancement of Artificial Intelligence (AAAI)*, 2018. 2, 4
- AI, A. Fuyu-8b: A multimodal architecture for AI agents, 2023. 6
- Alabdulmohsin, I. M., Zhai, X., Kolesnikov, A., and Beyer, L. Getting ViT in shape: Scaling laws for compute-optimal model design. *arXiv preprint arXiv:2305.13035*, 2023. 6
- Alayrac, J.-B., Donahue, J., Luc, P., Miech, A., Barr, I., Hasson, Y., Lenc, K., Mensch, A., Millican, K., Reynolds, M., Ring, R., Rutherford, E., Cabi, S., Han, T., Gong, Z., Samangooei, S., Monteiro, M., Menick, J., Borgeaud, S., Brock, A., Nematzadeh, A., Sharifzadeh, S., Binkowski, M., Barreira, R., Vinyals, O., Zisserman, A., and Simonyan, K. Flamingo: a visual language model for few-shot learning. In *Advances in Neural Information Processing Systems (NeurIPS)*, 2022. 9
- Bai, J., Bai, S., Yang, S., Wang, S., Tan, S., Wang, P., Lin, J., Zhou, C., and Zhou, J. Qwen-vl: A versatile vision-language model for understanding, localization, text reading, and beyond. *arXiv preprint arXiv:2308.12966*, 2023. 3
- Biderman, S., Schoelkopf, H., Anthony, Q. G., Bradley, H., O’Brien, K., Hallahan, E., Khan, M. A., Purohit, S., Prashanth, U. S., Raff, E., et al. Pythia: A suite for analyzing large language models across training and scaling. In *International Conference on Machine Learning (ICML)*, 2023. 3
- Bigham, J. P., Jayant, C., Ji, H., Little, G., Miller, A., Miller, R. C., Miller, R., Tatarowicz, A., White, B., White, S., and Yeh, T. VizWiz: nearly real-time answers to visual questions. In *User Interface Software and Technology (UIST)*, pp. 333–342, 2010. 2, 3, 10
- Brohan, A., Brown, N., Carbajal, J., Chebotar, Y., Chormanski, K., Ding, T., Driess, D., Finn, C., Florence, P. R., Fu, C., Arenas, M. G., Gopalakrishnan, K., Han, K., Hausman, K., Herzog, A., Hsu, J., Ichter, B., Irpan, A., Joshi, N. J., Julian, R. C., Kalashnikov, D., Kuang, Y., Leal, I., Levine, S., Michalewski, H., Mordatch, I., Pertsch, K., Rao, K., Reymann, K., Ryoo, M. S., Salazar, G., Sanketi, P. R., Sermanet, P., Singh, J., Singh, A., Soricut, R., Tran, H., Vanhoucke, V., Vuong, Q. H., Wahid, A., Welker, S., Wohlhart, P., Xiao, T., Yu, T., and Zitkovich, B. RT-2: Vision-language-action models transfer web knowledge to robotic control. *arXiv preprint arXiv:2307.15818*, 2023. 1, 9
- Brown, T. B., Mann, B., Ryder, N., Subbiah, M., Kaplan, J., Dhariwal, P., Neelakantan, A., Shyam, P., Sastry, G., Askell, A., Agarwal, S., Herbert-Voss, A., Krueger, G., Henighan, T., Child, R., Ramesh, A., Ziegler, D. M., Wu, J., Winter, C., Hesse, C., Chen, M., Sigler, E., Litwin, M., Gray, S., Chess, B., Clark, J., Berner, C., McCandlish, S., Radford, A., Sutskever, I., and Amodei, D. Language models are few-shot learners. *arXiv preprint arXiv:2005.14165*, 2020. 10
- Chen, K., Zhang, Z., Zeng, W., Zhang, R., Zhu, F., and Zhao, R. Shikra: Unleashing multimodal llms referential dialogue magic. *arXiv preprint arXiv:2306.15195*, 2023a. 5
- Chen, X., Wang, X., Beyer, L., Kolesnikov, A., Wu, J., Voigtlaender, P., Mustafa, B., Goodman, S., Alabdulmohsin, I. M., Padlewski, P., Salz, D. M., Xiong, X., Vlastic, D., Pavetic, F., Rong, K., Yu, T., Keysers, D., Zhai, X.-Q., and Soricut, R. PaLI-3 vision language models: Smaller, faster, stronger. *arXiv preprint arXiv:2310.09199*, 2023b. 2, 3
- Chung, H. W., Hou, L., Longpre, S., Zoph, B., Tay, Y., Fedus, W., Li, E., Wang, X., Dehghani, M., Brahma, S., Webson, A., Gu, S. S., Dai, Z., Suzgun, M., Chen, X., Chowdhery, A., Valter, D., Narang, S., Mishra, G., Yu, A. W., Zhao, V., Huang, Y., Dai, A. M., Yu, H., Petrov, S., Hsin Chi, E. H., Dean, J., Devlin, J., Roberts, A., Zhou, D., Le, Q. V., and Wei, J. Scaling instruction-finetuned language models. *arXiv preprint arXiv:2210.11416*, 2022. 7
- Dai, W., Li, J., Li, D., Tiong, A. M. H., Zhao, J., Wang, W., Li, B. A., Fung, P., and Hoi, S. C. H. InstructBLIP: Towards general-purpose vision-language models with instruction tuning. *arXiv preprint arXiv:2305.06500*, 2023. 19
- Dosovitskiy, A., Beyer, L., Kolesnikov, A., Weissenborn, D., Zhai, X., Unterthiner, T., Dehghani, M., Minderer, M., Heigold, G., Gelly, S., Uszkoreit, J., and Houshy, N. An image is worth 16x16 words: Transformers for image recognition at scale. In *International Conference on Learning Representations (ICLR)*, 2021. 3, 6, 18
- Driess, D., Xia, F., Sajjadi, M. S. M., Lynch, C., Chowdhery, A., Ichter, B., Wahid, A., Tompson, J., Vuong, Q. H., Yu, T., Huang, W., Chebotar, Y., Sermanet, P., Duckworth, D., Levine, S., Vanhoucke, V., Hausman, K., Toussaint, M., Greff, K., Zeng, A., Mordatch, I., and Florence, P. R. Palm-e: An embodied multimodal language model. In *International Conference on Machine Learning (ICML)*, 2023. 1, 5
- Gao, P., Han, J., Zhang, R., Lin, Z., Geng, S., Zhou, A., Zhang, W., Lu, P., He, C., Yue, X., Li, H., and Qiao, Y. J.

- Llama-adapter v2: Parameter-efficient visual instruction model. *arXiv preprint arXiv:2304.15010*, 2023. 18
- Gong, T., Lyu, C., Zhang, S., Wang, Y., Zheng, M., Zhao, Q., Liu, K., Zhang, W., Luo, P., and Chen, K. Multimodal-GPT: A vision and language model for dialogue with humans. *ArXiv*, 0, 2023. 1
- Goyal, Y., Khot, T., Summers-Stay, D., Batra, D., and Parikh, D. Making the V in VQA matter: Elevating the role of image understanding in visual question answering. In *Computer Vision and Pattern Recognition (CVPR)*, 2017. 2, 3, 17
- Gupta, A., Dollár, P., and Girshick, R. B. LVIS: A dataset for large vocabulary instance segmentation. In *Computer Vision and Pattern Recognition (CVPR)*, 2019. 8
- Hendrycks, D. and Gimpel, K. Gaussian error linear units (gelus). *arXiv preprint arXiv:1606.08415*, 2016. 18
- Hudson, D. A. and Manning, C. D. GQA: A new dataset for real-world visual reasoning and compositional question answering. In *Computer Vision and Pattern Recognition (CVPR)*, 2019. 2, 3, 17
- Jiang, A. Q., Sablayrolles, A., Mensch, A., Bamford, C., Chaplot, D. S., de Las Casas, D., Bressand, F., Lengyel, G., Lample, G., Saulnier, L., Lavaud, L. R., Lachaux, M.-A., Stock, P., Scao, T. L., Lavril, T., Wang, T., Lacroix, T., and Sayed, W. E. Mistral 7b. *arXiv preprint arXiv:2310.06825*, 2023. 2
- Karamcheti, S., Orr, L., Bolton, J., Zhang, T., Goel, K., Narayan, A., Bommasani, R., Narayanan, D., Hashimoto, T., Jurafsky, D., Manning, C. D., Potts, C., Ré, C., and Liang, P. Mistral - a journey towards reproducible language model training, 2021. 3
- Karamcheti, S., Nair, S., Chen, A. S., Kollar, T., Finn, C., Sadigh, D., and Liang, P. Language-driven representation learning for robotics. In *Robotics: Science and Systems (RSS)*, 2023. 7
- Kazemzadeh, S., Ordonez, V., Matten, M., and Berg, T. ReferItGame: Referring to objects in photographs of natural scenes. In *Empirical Methods in Natural Language Processing (EMNLP)*, pp. 787–798, 2014. 2, 4, 17
- Kerr, J., Kim, C. M., Goldberg, K., Kanazawa, A., and Tancik, M. LERF: Language embedded radiance fields. In *International Conference on Computer Vision (ICCV)*, 2023. 7
- Kobayashi, S., Matsumoto, E., and Sitzmann, V. Decomposing nerf for editing via feature field distillation. *arXiv preprint arXiv:2205.15585*, 2022. 7
- Krishna, R., Zhu, Y., Groth, O., Johnson, J., Hata, K., Kravitz, J., Chen, S., Kalantidi, Y., Li, L.-J., Shamma, D. A., Bernstein, M. S., and Li, F.-F. Visual genome: Connecting language and vision using crowdsourced dense image annotations. *International Journal of Computer Vision*, 123:32–73, 2017. 17
- Laurençon, H., Saulnier, L., Tronchon, L., Bekman, S., Singh, A., Lozhkov, A., Wang, T., Karamcheti, S., Rush, A. M., Kiela, D., Cord, M., and Sanh, V. OBELICS: An open web-scale filtered dataset of interleaved image-text documents. In *Neural Information Processing Systems Track on Datasets and Benchmarks (NeurIPS Datasets and Benchmarks)*, 2023. 9
- Li, B., Zhang, P., Yang, J., Zhang, Y., Pu, F., and Liu, Z. Otterhd: A high-resolution multi-modality model. *arXiv preprint arXiv:2311.04219*, 2023a. 6
- Li, J., Li, D., Xiong, C., and Hoi, S. C. H. BLIP: Bootstrapping language-image pre-training for unified vision-language understanding and generation. In *International Conference on Machine Learning (ICML)*, 2022. 2, 16, 17
- Li, J., Li, D., Savarese, S., and Hoi, S. C. H. BLIP-2: Bootstrapping language-image pre-training with frozen image encoders and large language models. In *International Conference on Machine Learning (ICML)*, 2023b. 2, 5
- Li, K., He, Y., Wang, Y., Li, Y., Wang, W., Luo, P., Wang, Y., Wang, L., and Qiao, Y. Videochat: Chat-centric video understanding. *ArXiv*, 0, 2023c. 1
- Li, X. L. and Liang, P. Prefix-tuning: Optimizing continuous prompts for generation. In *Association for Computational Linguistics (ACL)*, 2021. 18
- Li, Y., Du, Y., Zhou, K., Wang, J., Zhao, W. X., and rong Wen, J. Evaluating object hallucination in large vision-language models. In *Empirical Methods in Natural Language Processing (EMNLP)*, 2023d. 2, 4, 10
- Lin, T.-Y., Maire, M., Belongie, S., Hays, J., Perona, P., Ramanan, D., Dollár, P., and Zitnick, C. L. Microsoft COCO: Common objects in context. In *European Conference on Computer Vision (ECCV)*, pp. 740–755, 2014. 10, 17
- Liu, F., Emerson, G. E. T., and Collier, N. Visual spatial reasoning. *Transactions of the Association for Computational Linguistics (TACL)*, 11:635–651, 2022. 2, 4
- Liu, F., Lin, K., Li, L., Wang, J., Yacoob, Y., and Wang, L. Mitigating hallucination in large multi-modal models via robust instruction tuning. *arXiv preprint arXiv:2306.14565*, 2023a. 8, 16

- Liu, H., Li, C., Li, Y., and Lee, Y. J. Improved baselines with visual instruction tuning. *arXiv preprint arXiv:2310.03744*, 2023b. [1](#), [2](#), [3](#), [5](#), [6](#), [17](#), [18](#)
- Liu, H., Li, C., Wu, Q., and Lee, Y. J. Visual instruction tuning. In *Advances in Neural Information Processing Systems (NeurIPS)*, 2023c. [3](#), [17](#)
- Liu, X., Zhu, Y., Lan, Y., Yang, C., and Qiao, Y. Query-relevant images jailbreak large multi-modal models. *arXiv preprint arXiv:2311.17600*, 2023d. [10](#)
- Liu, Y., Duan, H., Zhang, Y., Li, B., Zhang, S., Zhao, W., Yuan, Y., Wang, J., He, C., Liu, Z., Chen, K., and Lin, D. MMBench: Is your multi-modal model an all-around player? *arXiv preprint arXiv:2307.06281*, 2023e. [3](#)
- Marino, K., Rastegari, M., Farhadi, A., and Mottaghi, R. OK-VQA: A visual question answering benchmark requiring external knowledge. In *Computer Vision and Pattern Recognition (CVPR)*, 2019. [17](#)
- Mishra, A., Shekhar, S., Singh, A. K., and Chakraborty, A. OCR-VQA: Visual question answering by reading text in images. In *International Conference on Document Analysis and Recognition (ICDAR)*, 2019. [17](#)
- OpenAI, Achiam, J., Adler, S., Agarwal, S., Ahmad, L., Akkaya, I., Aleman, F. L., Almeida, D., Altenschmidt, J., Altman, S., Anadkat, S., Avila, R., Babuschkin, I., Balaji, S., Balcom, V., Baltescu, P., Bao, H., Bavarian, M., Belgum, J., Bello, I., Berdine, J., Bernadett-Shapiro, G., Berner, C., Bogdonoff, L., Boiko, O., Boyd, M., Brakman, A.-L., Brockman, G., Brooks, T., Brundage, M., Button, K., Cai, T., Campbell, R., Cann, A., Carey, B., Carlson, C., Carmichael, R., Chan, B., Chang, C., Chantzis, F., Chen, D., Chen, S., Chen, R., Chen, J., Chen, M., Chess, B., Cho, C., Chu, C., Chung, H. W., Cummings, D., Currier, J., Dai, Y., Decareaux, C., Degry, T., Deutsch, N., Deville, D., Dhar, A., Dohan, D., Dowling, S., Dunning, S., Ecoffet, A., Eleti, A., Eloundou, T., Farhi, D., Fedus, L., Felix, N., Fishman, S. P., Forte, J., Fulford, I., Gao, L., Georges, E., Gibson, C., Goel, V., Gogineni, T., Goh, G., Gontijo-Lopes, R., Gordon, J., Grafstein, M., Gray, S., Greene, R., Gross, J., Gu, S. S., Guo, Y., Hallacy, C., Han, J., Harris, J., He, Y., Heaton, M., Heidecke, J., Hesse, C., Hickey, A., Hickey, W., Hoeschele, P., Houghton, B., Hsu, K., Hu, S., Hu, X., Huizinga, J., Jain, S., Jain, S., Jang, J., Jiang, A., Jiang, R., Jin, H., Jin, D., Jomoto, S., Jonn, B., Jun, H., Kaftan, T., Kaiser, L., Kamali, A., Kanitscheider, I., Keskar, N. S., Khan, T., Kilpatrick, L., Kim, J. W., Kim, C., Kim, Y., Kirchner, H., Kiros, J. R., Knight, M., Kokotajlo, D., Kondraciuk, L., Kondrich, A., Konstantinidis, A., Kosic, K., Krueger, G., Kuo, V., Lampe, M., Lan, I., Lee, T., Leike, J., Leung, J., Levy, D., Li, C. M., Lim, R., Lin, M., Lin, S., Litwin, M., Lopez, T., Lowe, R., Lue, P., Makanju, A. A., Malfacini, K., Manning, S., Markov, T., Markovski, Y., Martin, B., Mayer, K., Mayne, A., McGrew, B., McKinney, S. M., McLeavey, C., McMillan, P., McNeil, J., Medina, D., Mehta, A., Menick, J., Metz, L., Mishchenko, A., Mishkin, P., Monaco, V., Morikawa, E., Mossing, D. P., Mu, T., Murati, M., Murk, O., Mèly, D., Nair, A., Nakano, R., Nayak, R., Neelakantan, A., Ngo, R., Noh, H., Long, O., O’Keefe, C., Pachocki, J. W., Paino, A., Palermo, J., Pantuliano, A., Parascandolo, G., Parish, J., Parparita, E., Passos, A., Pavlov, M., Peng, A., Perelman, A., de Avila Belbute Peres, F., Petrov, M., de Oliveira Pinto, H. P., Pokorny, M., Pokrass, M., Pong, V. H., Powell, T., Power, A., Power, B., Proehl, E., Puri, R., Radford, A., Rae, J., Ramesh, A., Raymond, C., Real, F., Rimbach, K., Ross, C., Rotsted, B., Roussez, H., Ryder, N., Saltarelli, M. D., Sanders, T., Santurkar, S., Sastry, G., Schmidt, H., Schnurr, D., Schulman, J., Selsam, D., Sheppard, K., Sherbakov, T., Shieh, J., Shoker, S., Shyam, P., Sidor, S., Sigler, E., Simens, M., Sitkin, J., Slama, K., Sohl, I., Sokolowsky, B. D., Song, Y., Staudacher, N., Such, F. P., Summers, N., Sutskever, I., Tang, J., Tezak, N. A., Thompson, M., Tillet, P., Tootoonchian, A., Tseng, E., Tuggle, P., Turley, N., Tworek, J., Uribe, J. F. C., Vallone, A., Vijayvergiya, A., Voss, C., Wainwright, C., Wang, J. J., Wang, A., Wang, B., Ward, J., Wei, J., Weinmann, C., Welihinda, A., Welinder, P., Weng, J., Weng, L., Wiethoff, M., Willner, D., Winter, C., Wolrich, S., Wong, H., Workman, L., Wu, S., Wu, J., Wu, M., Xiao, K., Xu, T., Yoo, S., Yu, K., Yuan, Q., Zaremba, W., Zellers, R., Zhang, C., Zhang, M., Zhao, S., Zheng, T., Zhuang, J., Zhuk, W., and Zoph, B. GPT-4 technical report. *arXiv preprint arXiv:2303.08774*, 2023. [3](#), [17](#)
- Oquab, M., Darcet, T., Moutakanni, T., Vo, H. Q., Szafraniec, M., Khalidov, V., Fernandez, P., Haziza, D., Massa, F., El-Nouby, A., Assran, M., Ballas, N., Galuba, W., Howes, R., Huang, P.-Y. B., Li, S.-W., Misra, I., Rabbat, M. G., Sharma, V., Synnaeve, G., Xu, H., Jégou, H., Mairal, J., Labatut, P., Joulin, A., and Bojanowski, P. DINOv2: Learning robust visual features without supervision. *Transactions of Machine Learning Research (TMLR)*, 2023. [2](#), [6](#)
- Ordonez, V., Kulkarni, G., and Berg, T. L. Im2Text: Describing images using 1 million captioned photographs. In *Advances in Neural Information Processing Systems (NeurIPS)*, 2011. [17](#)
- Ouyang, L., Wu, J., Jiang, X., Almeida, D., Wainwright, C. L., Mishkin, P., Zhang, C., Agarwal, S., Slama, K., Ray, A., Schulman, J., Hilton, J., Kelton, F., Miller, L. E., Simens, M., Askell, A., Welinder, P., Christiano, P., Leike, J., and Lowe, R. J. Training language models to follow instructions with human feedback. *arXiv*, 2022. [7](#)
- Qi, X., Huang, K., Panda, A., Wang, M., and Mittal, P.

- Visual adversarial examples jailbreak aligned large language models. *arXiv preprint arXiv:2306.13213*, 2023. 10
- Radford, A., Kim, J. W., Hallacy, C., Ramesh, A., Goh, G., Agarwal, S., Sastry, G., Askell, A., Mishkin, P., Clark, J., Krueger, G., and Sutskever, I. Learning transferable visual models from natural language supervision. In *International Conference on Machine Learning (ICML)*, volume 139, pp. 8748–8763, 2021. 2, 4, 6
- Rasley, J., Rajbhandari, S., Ruwase, O., and He, Y. DeepSpeed: System optimizations enable training deep learning models with over 100 billion parameters. In *International Conference on Knowledge Discovery and Data Mining (KDD)*, 2020. 3
- Schuhmann, C., Vencu, R., Beaumont, R., Kaczmarczyk, R., Mullis, C., Katta, A., Coombes, T., Jitsev, J., and Komatsuzaki, A. LAION-400M: Open dataset of CLIP-filtered 400 million image-text pairs. *arXiv preprint arXiv:2111.02114*, 2021. 3, 10, 17
- Schwenk, D., Khandelwal, A., Clark, C., Marino, K., and Mottaghi, R. A-OKVQA: A benchmark for visual question answering using world knowledge. *arXiv preprint arXiv:2206.01718*, 2022. 17
- ShareGPT. ShareGPT, 2023. 3, 7, 17
- Sharma, P., Ding, N., Goodman, S., and Soricut, R. Conceptual captions: A cleaned, hypernymed, image alt-text dataset for automatic image captioning. In *Association for Computational Linguistics (ACL)*, 2018. 3, 17
- Sidorov, O., Hu, R., Rohrbach, M., and Singh, A. TextCaps: a dataset for image captioning with reading comprehension. In *European Conference on Computer Vision (ECCV)*, 2020. 3, 17
- Singh, A., Natarajan, V., Shah, M., Jiang, Y., Chen, X., Batra, D., Parikh, D., and Rohrbach, M. Towards VQA models that can read. In *Computer Vision and Pattern Recognition (CVPR)*, 2019. 2, 3
- Steiner, A., Kolesnikov, A., Zhai, X., Wightman, R., Uszkoreit, J., and Beyer, L. How to train your ViT? data, augmentation, and regularization in vision transformers. *Transactions of Machine Learning Research (TMLR)*, 2021. 6
- Subramanian, S., Narasimhan, M. G., Khangaonkar, K., Yang, K., Nagrani, A., Schmid, C., Zeng, A., Darrell, T., and Klein, D. Modular visual question answering via code generation. In *Association for Computational Linguistics (ACL)*, 2023. 1
- Sur’is, D., Menon, S., and Vondrick, C. ViperGPT: Visual inference via Python execution for reasoning. In *International Conference on Computer Vision (ICCV)*, 2023. 1, 9
- Tan, H. H. and Bansal, M. LXMERT: Learning cross-modality encoder representations from transformers. In *Empirical Methods in Natural Language Processing (EMNLP)*, 2019. 2
- Touvron, H., Martin, L., Stone, K. R., Albert, P., Almahairi, A., Babaei, Y., Bashlykov, N., Batra, S., Bhargava, P., Bhosale, S., Bikel, D. M., Blecher, L., Ferrer, C. C., Chen, M., Cucurull, G., Esiobu, D., Fernandes, J., Fu, J., Fu, W., Fuller, B., Gao, C., Goswami, V., Goyal, N., Hartshorn, A. S., Hosseini, S., Hou, R., Inan, H., Kardas, M., Kerkez, V., Khabsa, M., Kloumann, I. M., Korenev, A. V., Koura, P. S., Lachaux, M.-A., Lavril, T., Lee, J., Liskovich, D., Lu, Y., Mao, Y., Martinet, X., Mihaylov, T., Mishra, P., Molybog, I., Nie, Y., Poulton, A., Reizenstein, J., Rungta, R., Saladi, K., Schelten, A., Silva, R., Smith, E. M., Subramanian, R., Tan, X., Tang, B., Taylor, R., Williams, A., Kuan, J. X., Xu, P., Yan, Z., Zarov, I., Zhang, Y., Fan, A., Kambadur, M., Narang, S., Rodriguez, A., Stojnic, R., Edunov, S., and Scialom, T. Llama 2: Open foundations and fine-tuned chat models. *arXiv preprint arXiv:2307.09288*, 2023. 2, 7, 10
- Wang, J., Meng, L., Weng, Z., He, B., Wu, Z., and Jiang, Y.-G. To see is to believe: Prompting GPT-4V for better visual instruction tuning. *arXiv preprint arXiv:2311.07574*, 2023. 8
- Wang, K.-J., Liu, Y.-H., Su, H.-T., Wang, J.-W., Wang, Y.-S., Hsu, W. H., and Chen, W.-C. OCID-Ref: A 3d robotic dataset with embodied language for clutter scene grounding. In *Association for Computational Linguistics (ACL)*, 2021. 2, 4, 19
- Wightman, R. Pytorch image models. <https://github.com/rwightman/pytorch-image-models>, 2019. 3, 18
- Wolf, T., Debut, L., Sanh, V., Chaumond, J., Delangue, C., Moi, A., Cistac, P., Rault, T., Louf, R., Funtowicz, M., and Brew, J. HuggingFace’s transformers: State-of-the-art natural language processing. *arXiv preprint arXiv:1910.03771*, 2019. 3
- Ye, Q., Xu, H., Xu, G., Ye, J., Yan, M., Zhou, Y., Wang, J., Hu, A., Shi, P., Shi, Y., Li, C., Xu, Y., Chen, H., Tian, J., Qi, Q., Zhang, J., and Huang, F. mPLUG-Owl: Modularization empowers large language models with multimodality. *arXiv preprint arXiv:2304.14178*, 2023. 5, 18
- Yu, L., Poirson, P., Yang, S., Berg, A. C., and Berg, T. L. Modeling context in referring expressions. In *European*

Conference on Computer Vision (ECCV), 2016. [2](#), [4](#), [17](#), [19](#)

Yu, W., Yang, Z., Li, L., Wang, J., Lin, K., Liu, Z., Wang, X., and Wang, L. MM-Vet: Evaluating large multimodal models for integrated capabilities. *arXiv preprint arXiv:2308.02490*, 2023. [3](#)

Zellers, R., Holtzman, A., Rashkin, H., Bisk, Y., Farhadi, A., Roesner, F., and Choi, Y. Defending against neural fake news. In *Advances in Neural Information Processing Systems (NeurIPS)*, pp. 9054–9065, 2019. [10](#)

Zhai, X., Mustafa, B., Kolesnikov, A., and Beyer, L. Sigmoid loss for language image pre-training. In *International Conference on Computer Vision (ICCV)*, 2023. [6](#)

Zhao, Y., Gu, A., Varma, R., Luo, L., chin Huang, C., Xu, M., Wright, L., Shojanazeri, H., Ott, M., Shleifer, S., Desmaison, A., Balioglu, C., Nguyen, B., Chauhan, G., Hao, Y., and Li, S. PyTorch FSDP: Experiences on scaling fully sharded data parallel. In *Very Large Data Bases (VLDB)*, 2023. [2](#), [3](#), [18](#)

Zheng, L., Chiang, W.-L., Sheng, Y., Zhuang, S., Wu, Z., Zhuang, Y., Lin, Z., Li, Z., Li, D., Xing, E. P., Zhang, H., Gonzalez, J. E., and Stoica, I. Judging LLM-as-a-judge with MT-bench and chatbot arena. *arXiv preprint arXiv:2306.05686*, 2023. [7](#)

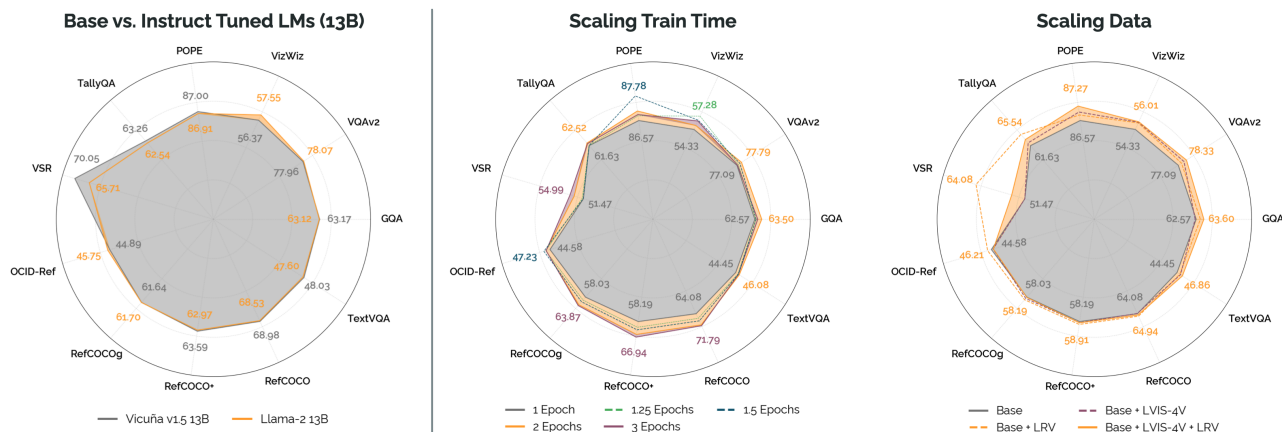


Figure 10. **Additional LM & Scaling Results.** We present additional results supplementing the investigations in §4.3 and §4.4. First, find that at the 13B parameter scale, base LMs perform comparably to instruct-tuned models (left). Next, we study how training time improves model performance. We find that evidence of severe *underfitting* at a single epoch, with performance improving until we hit two epochs, at which point performance plateaus (middle). Finally, we study the impact of scaling up data; adding data improves aggregate performance with the LRV-Instruct dataset (Liu et al., 2023a) having a more significant impact due to its increased image diversity (right).



Figure 11. **Qualitative Examples – Instruct-Tuned vs. Base LMs.** We find that base LMs (e.g., Llama-2) have slightly better qualitative performance compared to instruct-tuned LMs (e.g., Vicuña v1.5). Unsurprisingly, instruct-tuned LMs sometimes generate more verbose outputs. This verbosity can lead to *hallucinations*, such as in the monkey example on the left where the Vicuña v1.5 model incorrectly indicates that the man is also holding a knife. We additionally evaluate both models on an example from the BLIP-2 (Li et al., 2022) paper (right). We find that the base Llama-2 model gives a more accurate response, such as correctly identifying the Great Wall of China, going further to provide additional background information.

A. Training Visually-Conditioned Language Models

In the following sections, we provide additional detail around our VLM training procedure, including an expanded discussion of the LLaVa v1.5 pretraining datasets we use throughout our work, concrete implementation details for each component of the overarching VLM architecture, and hyperparameters for VLM training. All of the following information is also made explicit in our VLM training codebase.

A.1. Pretraining Dataset Composition

As described in §2, we use the LLaVa v1.5 (Liu et al., 2023b) pretraining datasets for the majority of our experiments. The dataset is comprised of two unique subsets, with each subset used for the multi-stage training procedure described in §4.1; during the first stage (“vision-language alignment”) only the projector F_ψ is trained, freezing the weights of the visual representation and LM. During the second stage (“multimodal instruct tuning”), both F_ψ and the LM are trained.

Vision-Language Alignment. The first subset consists of images sourced from LAION (Schuhmann et al., 2021), Conceptual Captions (CC; Sharma et al., 2018), and SBU Captions (SBU; Ordonez et al., 2011) augmented with synthetically generated captions from BLIP (Li et al., 2022), an early VLM optimized for captioning. As the goal of this first stage of training is simply to initialize the projector F_ψ , training is simple: given solely the image as input (e.g., no language prompt u_{prompt}), try and generate the corresponding caption; to update F_ψ we propagate gradients through the LM (freezing the weights). In total, this dataset consists of 558K (image, caption) pairs, where a caption is no longer than a sentence.

Multimodal Instruct Tuning. The second subset consists of 665K *multimodal instruct tuning examples*. In order to induce chat-like behavior and enable the VLM to perform specific tasks, Liu et al. (2023b) identify a set of “trigger prompts” u_{prompt} for each dataset in the mixture; these trigger prompts take the form of an instruction (e.g., “Describe the image.” or “Provide the bounding box coordinates for the region this sentence describes...”) with a corresponding target generation. The multimodal instruct tuning examples are sourced as follows:

LLaVa Synthetic Data (158K). A synthetically generated dataset of conversations, fine-grained descriptions, and question-answering data from Liu et al. (2023c), sourced by prompting GPT-4 (OpenAI et al., 2023) with image captions and object bounding boxes from COCO (Lin et al., 2014). Because this dataset was explicitly generated following the “instruct” format above, there is no need to define a separate trigger prompt.

Standard VQA Data (224K). A combination of visual question answering data sourced from the training sets of VQAv2 (general question answering; Goyal et al., 2017), GQA (spatial and compositional reasoning; Hudson & Manning, 2019), OK-VQA (reasoning requiring external knowledge; Marino et al., 2019), and OCR-VQA (reasoning over text/logos in images; Mishra et al., 2019). To encourage the VLM to generate responses of the appropriate format, LLaVa v1.5 defines the following trigger prompt: “(Question)? Answer the question using a single word or phrase.”

Multiple Choice VQA Data (50K). Multiple choice visual question answering data sourced from A-OKVQA (requires diverse external knowledge; Schwenk et al., 2022). As this is a multiple choice task, LLaVa v1.5 defines the following trigger prompt: “(Question)? A. (Option A) B. (Option B) ... Answer with the option’s letter from the given choices directly.”

Captioning Data (22K). Images and captions sourced from TextCaps (images with text/logos; Sidorov et al., 2020). LLaVa v1.5 defines the following trigger prompt: “Provide a one-sentence caption for the provided image.”

Referring Expression Data (116K). Referring expression grounding (bounding box prediction) and region captioning data sourced from RefCOCO (Kazemzadeh et al., 2014; Yu et al., 2016) and Visual Genome (Krishna et al., 2017). For bounding box prediction (localization), the model is tasked with producing *normalized bounding box coordinates* (as a natural language string). For the localization task, LLaVa v1.5 defines the following trigger prompt: “(Referring Expression) Provide the bounding box coordinates of the region this sentence describes.” For the inverse task (region caption), LLaVa v1.5 defines a separate trigger prompt: “Provide the bounding box coordinate of the region this sentence describes.”

ShareGPT (Language-Only) (40K). Language-only co-training data sourced from ShareGPT (ShareGPT, 2023), comprised of user-uploaded conversations with ChatGPT. Similar to the LLaVa Synthetic Data described above, this data is already in the expected “instruct” format, with no need for a separate trigger prompt.

A.2. Implementation – Architecture Components & Optimization

We implement our training codebase in PyTorch, leveraging its native Fully Sharded Data Parallel (FSDP; Zhao et al., 2023) implementation to distribute training across GPUs. We train all models in BF16 mixed precision. In the following section we provide additional details around each of the individual components of a VLM as described in §2.

Image Processing & Visual Representations. We implement all image processing logic using the default image transforms provided by torchvision and PyTorch Image Models (TIMM; Wightman, 2019). In addition to the resizing logic applied by the various schemes we evaluate in §4.2, we normalize pixel values using the defaults defined by each pretrained backbone (often the traditional ImageNet defaults).

The default backbone employed by all visual representation V_ω that we evaluate in this work is a Vision Transformer (ViT; Dosovitskiy et al., 2021); we extract patch features from the *penultimate* layer of the ViT, following the practice defined in LLaVa v1/v1.5 (Liu et al., 2023b).

Vision-Language Projector. While the projector F_ψ can be of arbitrary complexity, we opt to initialize a simple 2-layer GELU MLP (Hendrycks & Gimpel, 2016) that projects each patch independently into the embedding space of the LM.

Language Models. To combine projected patch “embeddings” output from F_ψ with the language prompt embeddings $E_\phi(u_{\text{prompt}})$ we perform simple sequence-wise concatenation, inserting the patch embeddings on the “left” of the prompt embeddings. This follows the process by many prior VLMs (Liu et al., 2023b; Ye et al., 2023; Gao et al., 2023), and is akin to prefix tuning (Li & Liang, 2021), where patch embeddings take the place of the randomly initialized prefix embeddings.

Prompting Base vs. Instruct-Tuned LMs. We use different prompting to accommodate instruct-tuned LMs (e.g., Vicuña v1.5) and base LMs (e.g., Llama-2). For Vicuña v1.5, we use the expected chat format, consisting of a system prompt and specially formatted “USER” and “ASSISTANT” blocks. We use the same system prompt adopted in LLaVa v1.5 – “A chat between a curious user and an artificial intelligence assistant. The assistant gives helpful, detailed, and polite answers to the user’s questions.” The template for prompt formatting is then:

```
<s>USER: {Input 1} ASSISTANT: {Response} <\s>
```

For the base LMs (e.g., Llama-2), we elide the system prompt entirely. We format examples as follows:

```
<s>In: {Input 1} Out: {Response} <\s>
```

A.3. Training Hyperparameters

We adopt the hyperparameters in Table 1 for *all* our single-stage experiments (for both 7B and 13B) models. For multi-stage pretraining (e.g., just for the experiments in Fig. 4) we increase the batch size to 256 and learning rate to 1e-3 when training the projector F_ψ for vision-language alignment; we keep all other hyperparameters the same.

Table 1. Training Hyperparameters

| Hyperparameter | Value |
|-------------------|-----------------------|
| Batch Size | 128 |
| Max Gradient Norm | 1.0 |
| Weight Decay | 0.1 |
| Learning Rate | 2e-5 |
| Optimizer | AdamW |
| Scheduler | Warmup & Cosine Decay |
| Warmup Ratio | 0.03 |

B. Evaluation Protocol

We provide additional details around our evaluation procedures, including how we prompt VLMs for evaluation tasks, how we compute metrics for each evaluation task, and finally, providing further detail around how we compute statistical significance when drawing conclusions. These procedures are also made explicit in our evaluation codebase.

B.1. Evaluation Procedures

Generating Responses. In order to run deterministic evaluations and fairly compare different models, we generate outputs via *greedy decoding*; we note that this ensures consistency, but may lead to worse quality outputs compared to using other LM generation strategies such as nucleus sampling or beam search.

Prompting VLMs for Individual Tasks. As evidenced by [Appx. A](#), different “trigger prompts” induce models to produce outputs of a specific structure (e.g., short phrases for visual question answering evaluations such as VQAv2). In our comparisons across models, we make sure to use the trigger prompts defined by the pretraining datasets, or in the original works. Specifically, we use the trigger prompts in [Appx. A](#) when evaluating our models and LLaVa v1.5, and those defined in [Dai et al. \(2023\)](#) for InstructBLIP.

Computing Evaluation Metrics. For all of our open-ended visual question answering tasks (VQAv2, TextVQA, GQA, and TextVQA), we report *accuracy* as computed by the official evaluation scripts. For TextVQA, we also run a variant of the evaluation where VLMs are additionally prompted with input tokens parsed by an OCR-system. These numbers *are only reported at the end of the appendices* ([Table 2](#)), and only to match the evaluation procedures used in the official LLaVa v1/v1.5 and InstructBLIP works. The TextVQA in the main body of the paper are run only assuming access to the image and question (without the OCR system inputs).

For our localization tasks, we report accuracy at the specific IoU thresholds defined in the official evaluations; for RefCOCO/RefCOCO+/RefCOCOg this is 0.5 IoU ([Yu et al., 2016](#)), while for OCID-Ref this is 0.25 IoU ([Wang et al., 2021](#)).

Finally, for challenge tasks, we format each example as a multiple choice question and report accuracy; for VSR and POPE this means two options (for True/False and Yes/No, respectively), and for TallyQA, sixteen (the numbers 0 - 15, inclusive).

B.2. Comparing Model Performance – Significance Testing

As addressed in [§4](#), each evaluation task uses different metrics, with different relative scales, making direct comparison challenging. We address this by computing normalized Z-scores for each model and evaluation (using the mean and standard deviation across all models), and compute global scores by averaging across all 12 benchmarks. To draw conclusions around the impact of a given design choice, we define two sets of models for comparison. The base set is reflective of the null hypothesis with the default configuration, while the alternate set is reflective of the new design choice. For each pair of models across the base and alternate sets, we compute the normalized performance difference, and perform a 1-sided Fisher T-test to compute significance ($p < 0.01$).

B.3. Exhaustive Results

For completeness, we tabulate evaluation results for all models trained in this work. Open-ended VQA results are in [Table 2](#), Localization results are in [Table 3](#), and Challenge Set results are in [Table 4](#).

Investigating the Design Space of Visually-Conditioned Language Models

Table 2. All Results on VQA Benchmarks

| Model | VQAv2 | GQA | VizWiz | TextVQA+OCR | TextVQA |
|--|-------|-------|--------|-------------|---------|
| Official Models | | | | | |
| LLaVa v1.5 7B | 76.54 | 61.58 | 54.24 | 58.25 | 46.13 |
| LLaVa v1.5 13B | 78.13 | 63.17 | 56.66 | 61.47 | 48.99 |
| InstructBLIP 7B | 76.12 | 48.41 | 32.02 | 28.01 | 33.54 |
| InstructBLIP 13B | 59.46 | 42.92 | 30.65 | 33.24 | 27.90 |
| Reproduction & Optimization Procedure | | | | | |
| LLaVa v1.5 7B (Reproduction) | 76.80 | 62.28 | 51.26 | 57.91 | 46.44 |
| LLaVa v1.5 13B (Reproduction) | 77.78 | 62.91 | 54.83 | 59.60 | 48.74 |
| Single-Stage 7B | 77.09 | 62.57 | 54.33 | 56.87 | 44.45 |
| Single-Stage 13B | 77.96 | 63.17 | 56.37 | 59.30 | 48.03 |
| Frozen ViT (Single-Stage) | 77.09 | 62.57 | 54.33 | 56.87 | 44.45 |
| Finetune ViT (Multi-Stage) | 74.36 | 60.08 | 57.27 | 56.56 | 44.40 |
| Finetune ViT (Single-Stage) | 73.53 | 59.65 | 55.26 | 53.81 | 38.33 |
| Visual Representation | | | | | |
| IN1K ViT-L 224px | 68.26 | 56.82 | 49.61 | 44.54 | 12.31 |
| DINOv2 ViT-L 224px | 66.29 | 55.64 | 48.37 | 44.70 | 12.62 |
| CLIP ViT-L 224px | 75.32 | 61.58 | 54.52 | 53.89 | 36.61 |
| SigLIP ViT-SO 224px | 76.32 | 62.15 | 58.82 | 55.75 | 40.50 |
| Image Preprocessing | | | | | |
| CLIP ViT-L 336px (Letterbox) | 77.09 | 62.57 | 54.33 | 56.87 | 44.45 |
| CLIP ViT-L 336px (Resize Crop) | 77.07 | 62.29 | 58.15 | 58.06 | 48.83 |
| CLIP ViT-L 336px (Naive Resize) | 77.86 | 63.48 | 56.03 | 59.09 | 49.66 |
| SigLIP ViT-SO 384px (Letterbox) | 78.61 | 63.39 | 56.88 | 60.33 | 52.71 |
| SigLIP ViT-SO 384px (Resize Crop) | 77.57 | 62.23 | 58.10 | 58.40 | 50.41 |
| SigLIP ViT-SO 384px (Naive Resize) | 78.81 | 63.60 | 57.47 | 61.06 | 54.87 |
| Visual Resolution Scaling | | | | | |
| CLIP ViT-L 224px | 75.32 | 61.58 | 54.52 | 53.89 | 36.61 |
| SigLIP ViT-SO 224px | 76.32 | 62.15 | 58.82 | 55.75 | 40.50 |
| CLIP ViT-L 336px | 77.09 | 62.57 | 54.33 | 56.87 | 44.45 |
| SigLIP ViT-SO 384px | 78.61 | 63.39 | 56.88 | 60.33 | 52.71 |
| Ensembling Visual Features | | | | | |
| CLIP 336px (Naive Resize) | 77.86 | 63.48 | 56.03 | 59.09 | 49.66 |
| DINOv2 + CLIP 336px (Letterbox) | 75.66 | 62.89 | 53.88 | 46.28 | 15.16 |
| DINOv2 + CLIP 336px (Naive Resize) | 75.90 | 63.57 | 55.31 | 46.20 | 15.67 |
| SigLIP 384px (Naive Resize) | 78.81 | 63.60 | 57.47 | 61.06 | 54.87 |
| DINOv2 + SigLIP 384px (Letterbox) | 78.66 | 63.81 | 59.00 | 58.77 | 50.11 |
| DINOv2 + SigLIP 384px (Naive Resize) | 79.18 | 64.33 | 61.06 | 60.31 | 52.18 |
| Base vs. Instruct Tuned LMs | | | | | |
| Vicuña v1.5 7B | 77.09 | 62.57 | 54.33 | 56.87 | 44.45 |
| Vicuña v1.5 13B | 77.96 | 63.17 | 56.37 | 59.30 | 48.03 |
| Llama-2 7B | 77.08 | 62.44 | 55.98 | 55.24 | 44.92 |
| Llama-2 13B | 78.07 | 63.12 | 57.55 | 58.42 | 47.60 |
| Co-training on Language Safety Data | | | | | |
| Vicuña v1.5 7B | 77.09 | 62.57 | 54.33 | 56.87 | 44.45 |
| Vicuña v1.5 7B (No Co-training) | 77.08 | 62.90 | 44.81 | 57.59 | 44.55 |
| Llama-2 7B | 77.08 | 62.44 | 55.98 | 55.24 | 44.92 |
| Llama-2 7B (No Co-training) | 77.10 | 62.94 | 43.60 | 56.04 | 45.45 |
| Scaling Train Time | | | | | |
| 1 Epoch | 77.09 | 62.57 | 54.33 | 56.87 | 44.45 |
| 1.25 Epochs | 77.30 | 62.70 | 57.28 | 57.22 | 45.44 |
| 1.5 Epochs | 77.54 | 62.75 | 56.37 | 56.42 | 45.63 |
| 2 Epochs | 77.79 | 63.50 | 55.20 | 56.12 | 46.08 |
| 3 Epochs | 77.17 | 62.96 | 56.20 | 54.01 | 45.69 |
| Scaling Data | | | | | |
| Base | 77.09 | 62.57 | 54.33 | 56.87 | 44.45 |
| Base + LRV | 77.58 | 63.13 | 55.76 | 57.23 | 45.67 |
| Base + LVIS-4V | 77.96 | 62.43 | 55.91 | 57.55 | 45.99 |
| Base + LVIS-4V + LRV | 78.33 | 63.60 | 56.01 | 59.06 | 46.86 |
| Prism 7B | | | | | |
| Prism-CLIP 7B (Controlled) | 77.87 | 63.65 | 56.10 | 58.40 | 50.31 |
| Prism-CLIP 7B | 79.67 | 64.56 | 53.34 | 57.72 | 51.12 |
| Prism-SigLIP 7B (Controlled) | 79.12 | 63.98 | 58.99 | 60.11 | 55.79 |
| Prism-SigLIP 7B | 80.67 | 64.32 | 53.70 | 62.14 | 58.01 |
| Prism-DINOSigLIP 7B (Controlled) | 79.05 | 64.16 | 59.82 | 58.69 | 51.78 |
| Prism-DINOSigLIP 7B | 80.97 | 65.27 | 52.82 | 59.71 | 55.64 |
| Prism 13B | | | | | |
| Prism-CLIP 13B (Controlled) | 78.83 | 64.10 | 57.09 | 61.10 | 52.22 |
| Prism-CLIP 13B | 80.38 | 65.07 | 56.47 | 61.56 | 53.40 |
| Prism-SigLIP 13B (Controlled) | 78.52 | 63.24 | 57.29 | 58.50 | 50.61 |
| Prism-SigLIP 13B | 80.68 | 64.56 | 57.63 | 60.09 | 54.28 |
| Prism-DINOSigLIP 13B (Controlled) | 80.07 | 65.14 | 56.61 | 61.20 | 54.10 |
| Prism-DINOSigLIP 13B | 81.66 | 66.13 | 58.01 | 62.89 | 57.08 |

Investigating the Design Space of Visually-Conditioned Language Models

Table 3. All Results on Localization Benchmarks

| Model | RefCOCO | RefCOCO+ | RefCOCOG | OCIDRef |
|--|---------|----------|----------|---------|
| Official Models | | | | |
| LLaVa v1.5 7B | 55.12 | 49.47 | 50.92 | 35.07 |
| LLaVa v1.5 13B | 66.75 | 61.36 | 60.85 | 45.56 |
| InstructBLIP 7B | N/A | N/A | N/A | N/A |
| InstructBLIP 13B | N/A | N/A | N/A | N/A |
| Reproduction & Optimization Procedure | | | | |
| LLaVa v1.5 7B (Reproduction) | 60.54 | 54.34 | 56.31 | 41.75 |
| LLaVa v1.5 13B (Reproduction) | 64.79 | 59.32 | 59.33 | 44.48 |
| Single-Stage 7B | 64.08 | 58.19 | 58.03 | 44.58 |
| Single-Stage 13B | 68.98 | 63.59 | 61.64 | 44.89 |
| Frozen ViT (Single-Stage) | 64.08 | 58.19 | 58.03 | 44.58 |
| Finetune ViT (Multi-Stage) | 19.24 | 17.48 | 23.12 | 16.35 |
| Finetune ViT (Single-Stage) | 42.56 | 37.89 | 41.05 | 33.42 |
| Visual Representations | | | | |
| IN1K ViT-L 224px | 43.24 | 35.40 | 36.05 | 19.58 |
| DINOv2 ViT-L 224px | 28.65 | 20.72 | 24.75 | 8.33 |
| CLIP ViT-L 224px | 59.88 | 53.69 | 53.37 | 37.16 |
| SigLIP ViT-SO 224px | 57.94 | 51.90 | 53.31 | 37.42 |
| Image Preprocessing | | | | |
| CLIP ViT-L 336px (Letterbox) | 64.08 | 58.19 | 58.03 | 44.58 |
| CLIP ViT-L 336px (Resize Crop) | 54.31 | 49.14 | 49.43 | 40.82 |
| CLIP ViT-L 336px (Naive Resize) | 65.28 | 58.79 | 59.93 | 44.20 |
| SigLIP ViT-SO 384px (Letterbox) | 63.09 | 56.24 | 58.17 | 45.50 |
| SigLIP ViT-SO 384px (Resize Crop) | 53.29 | 47.63 | 50.18 | 39.27 |
| SigLIP ViT-SO 384px (Naive Resize) | 61.38 | 55.76 | 56.84 | 41.49 |
| Visual Resolution Scaling | | | | |
| CLIP ViT-L 224px | 59.88 | 53.69 | 53.37 | 37.16 |
| SigLIP ViT-SO 224px | 57.94 | 51.90 | 53.31 | 37.42 |
| CLIP ViT-L 336px | 64.08 | 58.19 | 58.03 | 44.58 |
| SigLIP ViT-SO 384px | 63.09 | 56.24 | 58.17 | 45.50 |
| Ensembling Visual Features | | | | |
| CLIP ViT-L 336px (Naive Resize) | 65.28 | 58.79 | 59.93 | 44.20 |
| DINOv2 + CLIP 336px (Letterbox) | 72.44 | 65.84 | 64.32 | 47.41 |
| DINOv2 + CLIP 336px (Naive Resize) | 71.07 | 64.77 | 65.26 | 47.66 |
| SigLIP ViT-SO 384px (Naive Resize) | 61.38 | 55.76 | 56.84 | 41.49 |
| DINOv2 + SigLIP 384px (Letterbox) | 72.10 | 65.42 | 64.69 | 50.37 |
| DINOv2 + SigLIP 384px (Naive Resize) | 73.86 | 67.29 | 67.85 | 52.82 |
| Base vs. Instruct Tuned LMs | | | | |
| Vicuña v1.5 7B | 64.08 | 58.19 | 58.03 | 44.58 |
| Vicuña v1.5 13B | 68.98 | 63.59 | 61.64 | 44.89 |
| Llama-2 7B | 65.24 | 59.47 | 58.78 | 43.89 |
| Llama-2 13B | 68.53 | 62.97 | 61.70 | 45.75 |
| Co-training on Language Safety Data | | | | |
| Vicuña v1.5 7B | 64.08 | 58.19 | 58.03 | 44.58 |
| Vicuña v1.5 7B (No Co-training) | 63.94 | 57.51 | 57.88 | 44.11 |
| Llama-2 7B | 65.24 | 59.47 | 58.78 | 43.89 |
| Llama-2 7B (No Co-training) | 64.26 | 59.30 | 57.99 | 42.17 |
| Scaling Training Time | | | | |
| 1 Epoch | 64.08 | 58.19 | 58.03 | 44.58 |
| 1.25 Epochs | 67.02 | 61.37 | 60.01 | 46.45 |
| 1.5 Epochs | 68.62 | 62.81 | 61.21 | 47.23 |
| 2 Epochs | 71.23 | 65.40 | 63.32 | 46.32 |
| 3 Epochs | 71.79 | 66.94 | 63.87 | 46.25 |
| Scaling Data | | | | |
| Base | 64.08 | 58.19 | 58.03 | 44.58 |
| Base + LRV | 65.62 | 59.77 | 59.82 | 46.21 |
| Base + LVIS-4V | 63.91 | 58.82 | 58.91 | 43.83 |
| Base + LVIS-4V + LRV | 64.94 | 58.91 | 58.19 | 43.73 |
| Prism 7B | | | | |
| Prism-CLIP 7B (Controlled) | 66.42 | 60.14 | 60.56 | 44.12 |
| Prism-CLIP 7B | 71.98 | 66.96 | 66.18 | 44.65 |
| Prism-SigLIP 7B (Controlled) | 64.74 | 58.58 | 60.56 | 43.63 |
| Prism-SigLIP 7B | 70.92 | 65.73 | 65.46 | 48.08 |
| Prism-DINOSigLIP 7B (Controlled) | 73.62 | 67.85 | 66.34 | 50.56 |
| Prism-DINOSigLIP 7B | 77.78 | 73.08 | 71.04 | 54.12 |
| Prism 13B | | | | |
| Prism-CLIP 13B (Controlled) | 70.92 | 65.95 | 65.03 | 47.32 |
| Prism-CLIP 13B | 73.37 | 68.71 | 69.06 | 48.98 |
| Prism-SigLIP 13B (Controlled) | 59.21 | 53.33 | 54.66 | 40.44 |
| Prism-SigLIP 13B | 69.69 | 64.99 | 64.81 | 44.31 |
| Prism-DINOSigLIP 13B (Controlled) | 76.64 | 71.41 | 70.87 | 53.60 |
| Prism-DINOSigLIP 13B | 79.39 | 75.55 | 72.73 | 54.62 |

Investigating the Design Space of Visually-Conditioned Language Models

Table 4. All Results on Challenge Benchmarks

| Model | VSR | POPE | TallyQA |
|--|-------|-------|---------|
| Official Models | | | |
| LLaVa v1.5 7B | 51.47 | 86.57 | 62.06 |
| LLaVa v1.5 13B | 69.07 | 87.10 | 64.83 |
| InstructBLIP 7B | 58.92 | 84.30 | 15.51 |
| InstructBLIP 13B | 63.91 | 84.49 | 49.73 |
| Reproduction & Optimization Procedure | | | |
| LLaVa v1.5 7B (Reproduction) | 52.95 | 86.57 | 60.87 |
| LLaVa v1.5 13B (Reproduction) | 65.38 | 86.94 | 64.13 |
| Single-Stage 7B | 51.47 | 86.57 | 61.63 |
| Single-Stage 13B | 70.05 | 87.00 | 63.26 |
| Frozen ViT (Single-Stage) | 51.47 | 86.57 | 61.63 |
| Finetune ViT (Multi-Stage) | 57.20 | 82.70 | 59.15 |
| Finetune ViT (Single-Stage) | 51.47 | 83.82 | 59.53 |
| Visual Representations | | | |
| IN1K ViT-L 224px | 51.47 | 82.08 | 52.95 |
| DINOv2 ViT-L 224px | 51.47 | 84.84 | 57.12 |
| CLIP ViT-L 224px | 51.47 | 85.80 | 59.09 |
| SigLIP ViT-SO 224px | 51.47 | 85.07 | 63.02 |
| Image Preprocessing | | | |
| CLIP ViT-L 336px (Letterbox) | 51.47 | 86.57 | 61.63 |
| CLIP ViT-L 336px (Resize Crop) | 51.47 | 85.42 | 61.24 |
| CLIP ViT-L 336px (Naive Resize) | 51.47 | 87.01 | 62.90 |
| SigLIP ViT-SO 384px (Letterbox) | 51.47 | 86.78 | 64.83 |
| SigLIP ViT-SO 384px (Resize Crop) | 51.47 | 84.62 | 62.94 |
| SigLIP ViT-SO 384px (Naive Resize) | 51.47 | 86.52 | 65.47 |
| Visual Resolution Scaling | | | |
| CLIP ViT-L 224px | 51.47 | 85.80 | 59.09 |
| SigLIP ViT-SO 224px | 51.47 | 85.07 | 63.02 |
| CLIP ViT-L 336px | 51.47 | 86.57 | 61.63 |
| SigLIP ViT-SO 384px | 51.47 | 86.78 | 64.83 |
| Ensembling Visual Features | | | |
| CLIP 336px (Naive Resize) | 51.47 | 87.01 | 62.90 |
| DINOv2 + CLIP 336px (Letterbox) | 51.47 | 87.70 | 63.99 |
| DINOv2 + CLIP 336px (Naive Resize) | 51.47 | 87.29 | 65.02 |
| SigLIP 384px (Naive Resize) | 51.47 | 86.52 | 65.47 |
| DINOv2 + SigLIP 384px (Letterbox) | 51.47 | 87.89 | 67.19 |
| DINOv2 + SigLIP 384px (Naive Resize) | 51.55 | 88.30 | 67.63 |
| Base vs. Instruct Tuned LMs | | | |
| Vicuña v1.5 7B | 51.47 | 86.57 | 61.63 |
| Vicuña v1.5 13B | 70.05 | 87.00 | 63.26 |
| Llama-2 7B | 63.67 | 86.74 | 59.22 |
| Llama-2 13B | 65.71 | 86.91 | 62.54 |
| Co-training on Language Safety Data | | | |
| Vicuña v1.5 7B | 51.47 | 86.57 | 61.63 |
| Vicuña v1.5 7B (No Co-training) | 53.68 | 87.27 | 62.31 |
| Llama-2 7B | 63.67 | 86.74 | 59.22 |
| Llama-2 7B (No Co-training) | 67.18 | 86.88 | 57.17 |
| Scaling Training Time | | | |
| 1 Epoch | 51.47 | 86.57 | 61.63 |
| 1.25 Epochs | 51.80 | 86.80 | 61.69 |
| 1.5 Epochs | 51.55 | 87.78 | 61.67 |
| 2 Epochs | 53.93 | 87.03 | 62.52 |
| 3 Epochs | 54.99 | 86.86 | 62.30 |
| Scaling Data | | | |
| Base | 51.47 | 86.57 | 61.63 |
| Base + LRV | 64.08 | 86.84 | 65.54 |
| Base + LVIS-4V | 51.47 | 86.98 | 62.60 |
| Base + LVIS-4V + LRV | 54.91 | 87.27 | 63.74 |
| Prism 7B | | | |
| Prism-CLIP 7B (Controlled) | 66.61 | 86.83 | 60.86 |
| Prism-CLIP 7B | 57.77 | 87.30 | 66.00 |
| Prism-SigLIP 7B (Controlled) | 65.14 | 87.07 | 64.54 |
| Prism-SigLIP 7B | 56.79 | 87.30 | 66.46 |
| Prism-DINOSigLIP 7B (Controlled) | 66.28 | 88.28 | 65.07 |
| Prism-DINOSigLIP 7B | 59.57 | 88.12 | 66.70 |
| Prism 13B | | | |
| Prism-CLIP 13B (Controlled) | 65.96 | 86.96 | 65.71 |
| Prism-CLIP 13B | 71.85 | 87.23 | 69.37 |
| Prism-SigLIP 13B (Controlled) | 62.85 | 86.82 | 62.90 |
| Prism-SigLIP 13B | 64.57 | 87.50 | 68.95 |
| Prism-DINOSigLIP 13B (Controlled) | 71.85 | 88.50 | 66.09 |
| Prism-DINOSigLIP 13B | 72.18 | 88.07 | 70.41 |